

AD-A044 036

AEROSPACE CORP EL SEGUNDO CALIF SPACE SCIENCES LAB

F/6 4/1

SELF-CONSISTENT PARTICLE AND PARALLEL ELECTROSTATIC FIELD DISTR--ETC(U)

AUG 77 Y T CHIU, M SCHULZ

F04701-76-C-0077

UNCLASSIFIED

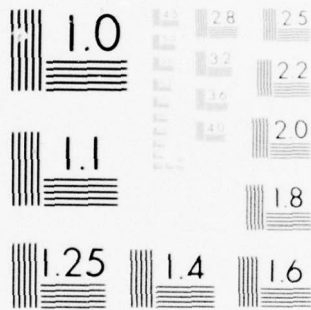
TR-0077(2960-04)-4

SAMSO-TR-77-156

NL

1 OF 1
AD 44036





MICROCOPY RESOLUTION TEST CHART
NATIONAL BUREAU OF STANDARDS-1963-A

AD A 044036

**Self-Consistent Particle and Parallel
Electrostatic Field Distributions
in the Magnetospheric-Ionospheric
Auroral Region**

Space Sciences Laboratory
The Ivan A. Getting Laboratories
The Aerospace Corporation
El Segundo, Calif. 90245

3 August 1977

Interim Report

APPROVED FOR PUBLIC RELEASE:
DISTRIBUTION UNLIMITED

Prepared for
SPACE AND MISSILE SYSTEMS ORGANIZATION
AIR FORCE SYSTEMS COMMAND
Los Angeles Air Force Station
P.O. Box 92960, Worldway Postal Center
Los Angeles, Calif. 90009

AD No.

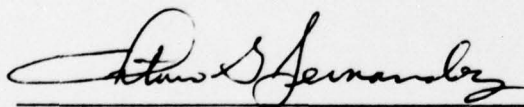
DDC FILE COPY

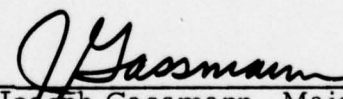
DDC
RECEIVED
SEP 12 1977
B

This interim report was submitted by The Aerospace Corporation, El Segundo, CA 90245, under Contract No. F04701-76-C-0077 with the Space and Missile Systems Organization, Deputy for Advanced Space Programs, P.O. Box 92960, Worldway Postal Center, Los Angeles, CA 90009. It was reviewed and approved for The Aerospace Corporation by G. A. Paulikas, Director, Space Sciences Laboratory. Lieutenant Dara Batki, SAMSO/YAPT, was the project officer for Advanced Space Programs.

This report has been reviewed by the Information Office (OI) and is releasable to the National Technical Information Service (NTIS). At NTIS, it will be available to the general public, including foreign nations.

This technical report has been reviewed and is approved for publication. Publication of this report does not constitute Air Force Approval of the report's findings or conclusions. It is published only for the exchange and stimulation of ideas.


for Dara Batki, 2nd Lt, USAF
Project Officer


Joseph Gassmann, Major, USAF

FOR THE COMMANDER


LEONARD E. BALTZELL, Col, USAF, Asst.
Deputy for Advanced Space Programs

UNCLASSIFIED

SECURITY CLASSIFICATION OF THIS PAGE (When Data Entered)

| REPORT DOCUMENTATION PAGE | | READ INSTRUCTIONS BEFORE COMPLETING FORM |
|--|--|--|
| 1. REPORT NUMBER 18 SAMSOTR-77-156 | 2. GOVT ACCESSION NO. | 3. RECIPIENT'S CATALOG NUMBER 9 |
| 4. TITLE (and Subtitle) 6 SELF-CONSISTENT PARTICLE AND PARALLEL ELECTROSTATIC FIELD DISTRIBUTIONS IN THE MAGNETOSPHERIC-IONOSPHERIC AURORAL REGION. | 5. TYPE OF REPORT & PERIOD COVERED Interim rept. | 6. PERFORMING ORG. REPORT NUMBER 14 TR-0077(2960-04)-4 ✓ |
| 7. AUTHOR(s) 10 Yam T. / Chiu Michael Michael / Schulz | 8. CONTRACT OR GRANT NUMBER(s) 15 F04701-76-C-0077 ✓ | |
| 9. PERFORMING ORGANIZATION NAME AND ADDRESS The Aerospace Corporation El Segundo, Calif. 90245 | 10. PROGRAM ELEMENT, PROJECT, TASK AREA & WORK UNIT NUMBERS | |
| 11. CONTROLLING OFFICE NAME AND ADDRESS Space and Missile Systems Organization Air Force Systems Command Los Angeles, Calif. 90009 | 12. REPORT DATE 11 3 Aug 77 ✓ | |
| 14. MONITORING AGENCY NAME & ADDRESS (if different from Controlling Office) | 13. NUMBER OF PAGES 71 12 75p | |
| | 15. SECURITY CLASS. (of this report) Unclassified | |
| 16. DISTRIBUTION STATEMENT (of this Report) Approved for public release; distribution unlimited | | |
| 17. DISTRIBUTION STATEMENT (of the abstract entered in Block 20, if different from Report) | | |
| 18. SUPPLEMENTARY NOTES | | |
| 19. KEY WORDS (Continue on reverse side if necessary and identify by block number) Aurora Electric Fields Ionosphere-Magnetosphere Interactions Particle Precipitation | | |
| 20. ABSTRACT (Continue on reverse side if necessary and identify by block number) The variation of the self-consistent electrostatic potential along the magnetic field is calculated by application of the principle of quasi-neutrality to the plasma components distributed along an auroral field line. The equilibrium plasma consists of hot anisotropic magnetospheric plasma, ionospheric plasma evaporated or extracted upwards by the parallel electrostatic field, and back-scattered electrons. It is shown that the above charged-particle populations can support a potential difference of up to several kilovolts between the equator and the ionosphere along an auroral field line. Moreover, the corresponding → next page | | |

DD FORM 1473
(FACSIMILE)

407512

UNCLASSIFIED
SECURITY CLASSIFICATION OF THIS PAGE (When Data Entered)

UNCLASSIFIED

SECURITY CLASSIFICATION OF THIS PAGE(When Data Entered)

19. KEY WORDS (Continued)

20. ABSTRACT (Continued)

parallel electric field has the proper signature to account for electron precipitation characteristics. Comparisons between theoretical and observed electron precipitation fluxes lead to estimates for the various physical parameters in the model.

| | |
|---------------------------------|---|
| ACCESSION for | |
| NTIS | White Section <input checked="" type="checkbox"/> |
| DDC | Buff Section <input type="checkbox"/> |
| UNANNOUNCED | <input type="checkbox"/> |
| JUSTIFICATION | |
| BY | |
| DISTRIBUTION/AVAILABILITY CODES | |
| Dist. and/or SPECIAL | |
| A | |

UNCLASSIFIED

SECURITY CLASSIFICATION OF THIS PAGE(When Data Entered)

PREFACE

We appreciate communications and/or discussions with Drs. J. M. Cornwall, D. S. Evans, J. F. Fennell, J. H. Hoffman, J. Lemaire, J. M. Luhmann, P. F. Mizera, A. L. Vampola, and J. D. Winningham.

CONTENTS

| | |
|----------------------------------|----|
| PREFACE | 1 |
| INTRODUCTION | 9 |
| QUASI-NEUTRALITY | 15 |
| PARTICLE POPULATIONS | 23 |
| THE MODEL | 39 |
| RESULTS | 47 |
| CONCLUSION | 63 |
| APPENDIX A: ACCESSIBILITY | 71 |
| APPENDIX B: DENSITY MOMENT | 71 |
| REFERENCES | 75 |

TABLES

| | | |
|----|---|----|
| 1. | Parameters of the Model | 45 |
| 2. | Parameters of the Fit | 48 |
| 3. | Parameters Yielding Solutions | 55 |

PRECEDING PAGE BLANK-NOT FILMED

FIGURES

1. The regions of phase space occupied by the various particle populations are shown schematically for (a) ions and for (b) electrons 37
2. Electron flux at 45° pitch angle observed in the day-side cusp region on 11 January 1975 on board the Tordo Dos rocket (Winningham et al., 1977) is shown as function of electron energy 41
3. Electron energy fluxes at 0° and at 180° pitch angles observed in an "inverted-V" structure (Mizera et al., 1976) are shown as functions of electron energy 42
4. The self-consistent electrostatic potential computed for the case corresponding to the observed electron flux of Figure 2 (Case W) is shown as function of magnetic-field ratio and altitude 51
5. The self-consistent electrostatic potential computed for the case corresponding to the observed electron flux of Figure 3 (Case M) is shown as function of magnetic-field ratio and altitude 52
6. Distributions of the various energetic particles along the field line, computed for Case W, are shown as functions of magnetic-field ratio 59
7. Distributions of the various "low-energy" particles along the field line, computed for Case W, are shown as functions of magnetic-field ratio 60

INTRODUCTION

Nearly two decades of magnetospheric research have established that charged particles from the solar wind are energized inside the magnetosphere, although the mechanism of their energization is not yet precisely determined. Hot magnetospheric plasma are often observed (DeForest and McIlwain, 1971; and references therein) in the equatorial region on auroral field lines. Observations of energetic electrons at low altitudes on the same auroral field lines (Evans, 1975; and references therein) and, more recently, observations of energetic ions of ionospheric origin (Hultqvist et al., 1971; Shelley et al., 1976; Mizera et al., 1976) confirm that magnetospheric and ionospheric plasmas interact strongly in the auroral region. In particular, beam-like pitch-angle and energy distributions are often observed and seem to indicate that such energetic particles have been accelerated or retarded by an electric field \vec{E} parallel to the magnetic field \vec{B} . Moreover, it has been pointed out (Evans, 1975) that the characteristics of such energetic electron events may perhaps be roughly classified into two categories: (a) transient events for which the flux distributions indicate diffusive energy gain, and (b) quiescent quasi-static events for which the pitch-angle and flux distributions show a beam-like behavior. Since the magnetospheric plasma during a substorm event is highly disturbed, the existence of the first category of event is not at all surprising; the diffusive energy gain might be associated with the anomalous resistance that can occur along a magnetic field line as consequence of several instability mechanisms (e.g., Perkins, 1968; Kindel and Keane, 1971; Papadopoulos and Coffey, 1974). The

second category of event, which does not show diffusive energy gain, seems to require a quasi-static electric potential difference of up to several kilovolts between the ionosphere and the equator in order to account for the beam-like behavior of electron flux distributions. Although a parallel electric field can arise as the result of mapping perpendicular electric fields downward into the ionosphere, where collisional resistance along and collisional conductance across the magnetic field may become important (Chiu, 1974), such a process is limited to the lower ionosphere and cannot account for the beam-like characteristics of energetic-electron precipitation. In regions of open field lines, charge-separation effects related to the polar wind also give rise to a parallel electric field (Banks and Holzer, 1968); however, the magnitude of such a total potential drop is far less than the potential differences of up to several kilovolts that are inferred to occur between the ionosphere and the equator along certain (presumably closed) auroral field lines. Thus, the evident existence of quasi-static parallel electric fields in the auroral region remains a puzzle in auroral physics. In this paper we propose to consider the origin of such parallel electrostatic fields and their mutual consistency with auroral plasma.

Basically, there are two mechanisms by which a quasi-static electric potential difference V_{\parallel} can be established along a magnetic field line in a collisionless plasma. On the one hand, one can appeal to quasi-stable double layers that have been produced in bounded laboratory plasmas (Quon and Wong, 1976) in which there are interpenetrating plasma streams involving ions and

electrons reflected from the walls. Although it has been conjectured (Block, 1975) that such double layers may also exist in the magnetosphere, where plasma boundaries are somewhat amorphous, we shall temporarily defer consideration of the double-layer mechanism until its existence and stability can be verified for magnetospheric plasma. On the other hand, Alfvén and Fälthammar (1963, pp. 163-167) have pointed out that an anisotropic collisionless plasma in a magnetic field can be in quasi-neutral equilibrium without a parallel electric field only if the magnetic field is homogeneous or if the pitch-angle anisotropy is the same for both electrons and ions. Otherwise, in the case of a dipolar magnetic field such as the earth's, the absence of a parallel electric field would result in different distributions of ions and electrons along the field line if the equatorial anisotropies of the particles were different. Conversely, charge neutrality of the plasma along the magnetic field line demands that an electrostatic field be established parallel to the magnetic field line. The electrostatic potential energy difference $|e|V_\ell$ between the ionosphere (where $B = B_\ell$) and the equator (where $B = B_0$) is estimated to be of the order of the mirror ratio B_ℓ/B_0 multiplied by the mean perpendicular particle energy (Alfvén and Fälthammar, 1963; Persson, 1966), i. e., to be of the order of hundreds of keV for plasma in an auroral flux tube. However, the magnetospheric-ionospheric flux tube along an auroral field line contains not only anisotropic magnetospheric plasma, but also thermal plasma extracted or evaporated from the ionosphere and back-scattered electrons of intermediate energy. Since the various components

of colder plasma (here assumed isotropic at the foot of the field line) are expected to participate in the maintenance of charge neutrality, we would expect the above estimates of electrostatic potential difference along an auroral field line (Alfvén and Fälthammar, 1963; Persson, 1966) to be unrealistically large. Indeed, calculations of the parallel electric field by application of the principle of quasi-neutrality (Lemaire and Scherer, 1973) yielded electrostatic potential differences of only a few volts between the ionosphere and the equator, although the effects of backscattered electrons and of pitch-angle anisotropy for magnetospheric plasma were ignored in those calculations. In view of the importance of the question, we have undertaken to re-examine the conditions which define quasi-neutrality for auroral plasma, especially for flux tubes in the high latitude trough region of the ionosphere, poleward of the plasmapause, where the energetic electron observations have been made.

In this paper, we apply the principle of quasi-neutrality to calculate the mutually consistent electrostatic potential and particle distributions along an auroral field line which is populated by collisionless anisotropic magnetospheric plasma and by plasma extracted or backscattered from the ionosphere. It is shown that a potential difference of up to several kilovolts between the equator and the ionosphere may thus be maintained along an auroral field line. While the parallel electric field has the proper signature to account for electron precipitation characteristics (Evans, 1975), it also may self-consistently account for the presence of O^+ ions with keV energies at the upper reaches of auroral field lines (Shelley et al., 1976).

Even though our calculation is similar to that of Lemaire and Scherer (1973, 1977), there are a number of crucial differences which combine to yield a larger potential drop along the field line in our work than in theirs. Among these, three essential factors peculiar to auroral field lines in the trough region are most important in accounting for the differences; indeed these may also explain why the beam-like characteristics of energetic particles are not observed elsewhere. First, as has been pointed out by Alfvén and Fälthammar (1963), different anisotropies for electrons and protons are crucial to the maintenance of a large potential drop along the field line. Since ring-current particles injected onto the auroral field line are expected to be anisotropic in pitch angle, we preserve such a feature in our calculation. Second, copious backscattered electrons are observed and must be considered in a quasi-neutrality calculation. Third, the number density of thermal ions at the ionosphere is an important boundary condition on the problem, since the ions are accelerated upward by the same parallel electric field that accounts for downward acceleration of electrons. Since the trough region of the ionosphere is considerably depleted relative to the average ionosphere, it is expected that the effect of the ionospheric plasma, which has a tendency to reduce the potential difference along a magnetic field line, is correspondingly minimized.

We shall show that in our model the energetic electron flux and pitch-angle distributions at the foot of the field line are essentially similar to those found in the previous model (Evans, 1975) for electron precipitation under the influence of arbitrarily postulated parallel electric fields.

In our calculation, however, we require that the electrostatic potential be a solution to the quasi-neutrality equation, and this requirement is found to be an important constraint on the admissibility of the electrostatic potential, otherwise postulated, for the problem. It should be noted that our approach, though yielding similar flux distributions at the foot of the field line, is basically different from Evans' approach. In Evans' model, the beam-like characteristics of precipitating electrons are attributed to the collimation of an isotropic electron population by an arbitrarily imposed parallel electric field. In our model, the parallel electric field arises naturally as a consequence of the quasi-neutrality requirement imposed on the various particle populations, some of which are assumed to be anisotropic at the equator. Thus, the mapping relationships between electron anisotropy and parallel electric field for the two models are different.

QUASI-NEUTRALITY

The principle of quasi-neutrality is commonly employed in problems of the present type (e.g., Lemaire and Scherer, 1973). One considers a dipolar magnetic flux tube in which the magnitude of \vec{B} varies monotonically from B_0 at the equator to B_l at the foot, which is located at an appropriate altitude to be discussed below. We construct a kinetic model in which the ion and electron distribution functions, f_+ and f_- , are expressed analytically in terms of the velocity components v_\perp and v_\parallel relative to \vec{B} , in terms of the local electrostatic potential $V_s \equiv V(s)$, and in terms of the local magnetic intensity $B_s \equiv B(s)$, where s is the coordinate that measures arc length of the field line from the equator. The principle of quasi-neutrality asserts that

$$\int_0^\infty v_\perp dv_\perp \int_{-\infty}^{+\infty} [f_+(v_\parallel, v_\perp; V_s) - f_-(v_\parallel, v_\perp; V_s)] dv_\parallel = 0. \quad (1)$$

For our model, in which f_+ and f_- are explicitly constructed, we interpret (1) as an equation for the value of V_s at any point s along the field line ($0 \leq s \leq l$) under the convention that V vanishes at the equator (i.e., $V_0 = 0$). Persson (1966) has shown that a necessary and sufficient condition for V to vanish at all points along the field line is for f_+ and f_- to have the same anisotropy, i.e., the same equatorial pitch-angle distribution. Since ring-current electrons and protons are believed to be

scattered in pitch angle by different wave modes (Kennel and Petschek, 1966; Cornwall, 1966), we expect that their pitch-angle distributions are not the same. Thus, an electrostatic potential $V_g \neq 0$ is required in order to satisfy the quasi-neutrality condition expressed by (1).

Since our model is intended for application in the topside ionosphere and the magnetosphere, the plasma is assumed to be collisionless in the interval $0 \leq s \leq l$. This assumption of collisionless plasma in the flux tube entails at least two consequences which require consideration at the outset. On the one hand, the distribution functions f_+ and f_- are required to be mapped along the field line in accordance with Liouville's theorem, the detailed consequences of which will be discussed below. On the other hand, we are obligated to select l so that all the charged-particle populations are indeed collisionless throughout the interval $0 \leq s \leq l$. For the magnetospheric proton population, which is obviously collisionless in the equatorial region of the auroral field line, the dominant collisional process in the ionosphere, where the neutral-particle density greatly exceeds the plasma density, is ion-neutral charge exchange. The collision time for this process is given by $t = 1/n_0 \sigma v$, where n_0 is the neutral-particle density, σ is the ion-neutral charge-exchange cross section, and v is the magnitude of the relative impact velocity. For hot magnetospheric plasma one identifies v with the speed of the charged particle and requires that the particle

be relatively free of collisions over its full bounce period $2\pi/\Omega_2 \sim 5LR_E/v$. Thus, the level corresponding to $s = \ell$ is to be determined from the condition that

$$\Omega_2 t \sim 2\pi/[5n_0(\ell)\sigma LR_E] \sim 1. \quad (2)$$

Using an average CIRA (1972) model of the neutral atmosphere and a representative value ($\approx 10^{-15} \text{ cm}^2$) for the proton-neutral charge-exchange cross section σ , we determine that the location $s = \ell$ corresponds to an altitude ~ 2000 km. The corresponding thermal plasma density at $s = \ell$ in the auroral region is extremely variable, since sharp ionospheric troughs are not limited to the plasmapause region (Hoffman et al., 1974). At high invariant latitudes ($> 65^\circ$), the trough ionospheric densities may be as low as 10^2 - 10^3 cm^{-3} in the nightside ionosphere and as high as 10^4 cm^{-3} in the dayside ionosphere at the 1400 km altitude (Hoffman et al., 1974). While the criterion (2) assures us that magnetospheric ions will be relatively free of charge-exchange collisions on their bounce time scale in the interval $0 \leq s \leq \ell$, charge-exchange collisions near the foot of the field line may exert sufficient frictional force on H^+ ions of ionospheric origin to modify their density distribution along the field line. We acknowledge that most energetic electrons, as well as ions with energies ≥ 50 keV, remain collisionless to much lower altitudes than 2000 km. It is a shortcoming

of our model that all particles going beyond $s = \ell$ are considered lost. This shortcoming could be remedied only by allowing ℓ to depend upon particle species and energy, but such a remedy would render the present model entirely intractable.

Having defined the interval $0 \leq s \leq \ell$ for which our model applies, we next consider the consequences of Liouville's theorem. Since the plasma is considered to be collisionless throughout the interval $0 \leq s \leq \ell$, the time-independent distribution function for either species must depend only on the constants of the motion, namely

$$W \equiv (m_q/2) (v_{\parallel s}^2 + v_{\perp s}^2) + q|e|V_s \quad (3)$$

and

$$\mu \equiv m_q v_{\perp s}^2 / 2B_s, \quad (4)$$

where m_q is the particle mass and $q(= \pm 1)$ is the particle charge in units of the electronic charge $|e|$. Liouville's theorem asserts that

$$f_{\pm}(v_{\parallel s}, v_{\perp s}; V_s) = f_{\pm}(v_{\parallel s'}, v_{\perp s'}; V_{s'}) \quad (5)$$

if the points $(v_{\parallel s}, v_{\perp s}; s)$ and $(v_{\parallel s'}, v_{\perp s'}; s')$ are connected by a dynamical trajectory in phase space. The conservation laws expressed by (3) and (4) imply that

$$v_{\parallel s'}^2 = v_{\parallel s}^2 + [1 - (B_{s'}/B_s)]v_{\perp s}^2 + (2q|e|/m_q)(V_s - V_{s'}) \quad (6)$$

for any such pair of points on the same dynamical trajectory in phase space. Thus, we say that the point $(v_{\parallel s}, v_{\perp s}; s)$ is accessible from the source point, defined as $(v_{\parallel s^*}, v_{\perp s^*}, s^*)$, if $v_{\parallel s'}$ is real (i.e., if $v_{\parallel s'}^2 > 0$) for all s' between s and s^* . An obviously necessary condition for particle accessibility to s from a source point s^* is that $v_{\parallel s^*}^2$, as given by (6), be positive or zero. The sufficiency of this condition, namely $v_{\parallel s^*}^2 \geq 0$, depends on the functional form of V_s . It can be shown (see Appendix A) that the condition $v_{\parallel s^*}^2 \geq 0$ is sufficient for accessibility to any source point s^* for both species of particle ($q = \pm 1$) if $dV_{s'}/dB_{s'} > 0$ and

$$(d^2V_{s'}/dB_{s'}^2) \leq 0 \quad (7)$$

for all points s' between s and s^* . In our model, we use the criterion $v_{\parallel s^*}^2 \geq 0$ to determine particle accessibility to their respective source points s^* ; thus, we require, in accordance with (7), that V_s increase monotonically with B_s and appear concave downward when plotted as a function of B_s throughout the entire interval $B_0 \leq B_s \leq B_\ell$. Since the functional form of V_s becomes evident only

upon solution of (1), we have to assume that the above requirements on dV_s/dB_s and d^2V_s/dB_s^2 are satisfied in specifying analytical forms for $f_{\pm}(v_{\parallel s}, v_{\perp s}; V_s)$ in our model. Only after "evaluation" of the density moment and "solution" of (1) for V_s are the derivatives dV_s/dB_s and d^2V_s/dB_s^2 available to be tested for sign. These conditions thus turn out to be very restrictive constraints (applied a posteriori) on the acceptability of "solutions" to (1). In theory, any "solution" of (1) not satisfying these constraints has to be discarded, since it would have been based on a false mapping of f_{\pm} in (1). In practice, however, a slight violation of (7) comparable to the limit of numerical resolution in computing the density moments may have to be tolerated.

A proper consideration of constraints upon V_s , based on accessibility of a particle to its source point in phase space, should include not only the electrostatic potential, as in (7), but also the gravitational potential. We have chosen to neglect the effects of gravity in (7) because we seek solutions for which $|e|V_{\ell} \sim 1$ keV. For O^+ ions, the gravitational escape energy from the 2000 km altitude is ~ 8.2 eV; therefore, we should have included the gravitational potential in the consideration of phase-space accessibility of cold ions near the foot of the field line where $|e|(V_{\ell} - V_s) \lesssim 10$ eV. We have properly included the gravitational potential in the treatment of the dynamics of cold ions, as was done in the works of Eviatar et al. (1964) and Lemaire and Scherer (1973). However, the enforcement of (7) as a constraint upon V_s near the foot

of the field line may not be sufficient, i.e., may constitute an erroneous allocation of points $(v_{\parallel}, v_{\perp}; s)$ in phase space with respect to accessibility of cold ions from their source point $s^* = l$. We have been able to show that, even if gravity is taken into consideration, cold ions satisfying $v_{\parallel s^*}^2 > 0$ in (6) are accessible to their source at the foot of the field line if V_s satisfies (7) and if dV_s/dB_s is sufficiently large near the foot of the field line (see Appendix A).

In the foregoing, we have concentrated on discussing the properties of V_s imposed by the requirement that the particles in phase space be accessible along dynamical trajectories to their sources, which are assumed to be either at the equator ($s^* = 0$) or at the foot of the field line ($s^* = l$). Among the possible particle populations supporting V_s , there may be populations which are not accessible to any source points in the interval $0 \leq s \leq l$ (Lemaire and Scherer, 1971 a; b). Such particles execute dynamical trajectories with two turning points in the interval $0 < s < l$, and are therefore trapped by the electrostatic potential on the one hand and by the effective magnetic mirroring potential on the other. For a potential V_s ($0 \leq V_s \leq V_l$) satisfying the constraint imposed by (7), only electrons may execute such trapped trajectories. We assume that the phase-space trajectories available for such trapped electrons are defined by the requirements that $v_{\parallel 0}^2 < 0$ and $v_{\parallel l}^2 < 0$.

Details on the construction of the model particle distribution functions for the various populations are given in the next section.

PARTICLE POPULATIONS

In the present model, the following plasma-constituent distributions are assumed to be present in the collisionless interval ($0 \leq s \leq l$) of the auroral flux tube: hot anisotropic magnetospheric plasma, $f_{Mq}(v_{\parallel s}, v_{\perp s}; V_s)$; cold thermal ionospheric plasma, $f_{Iq}(v_{\parallel s}, v_{\perp s}; V_s)$; two populations of backscattered electrons, $f_{Si}(v_{\parallel s}, v_{\perp s}; V_s)$ with ($i = 1, 2$); and trapped electrons, $f_T(v_{\parallel s}, v_{\perp s}; V_s)$. The magnetospheric distributions f_{Mq} are considered to arise from an equatorial source ($s^* = 0$) while the ionospheric distribution f_{Iq} and the backscattered distributions f_{Si} are considered to be injected at $s = l$. The trapped electrons f_T are considered to have been scattered into their trapped trajectories and do not require an accessible source.

Particles belonging to f_{Mq} are classified as precipitating ($v_{\parallel l}^2 > 0$) or mirroring ($v_{\parallel l}^2 < 0$) according to their respective values of

$$v_{\parallel l}^2 = v_{\parallel s}^2 + [1 - (B_l/B_s)]v_{\perp s}^2 + (2q|e|/m_q)(V_s - V_l), \quad (8)$$

which determines accessibility to $s = l$. Since v_{\parallel} is positive for down-going particles in our convention, and since all magnetospheric particles going beyond $s = l$ are considered to be absorbed, we require that $f_{M\pm} = 0$ for trajectories that obey both the condition $v_{\parallel} < 0$ and the condition $v_{\parallel l}^2 > 0$. Further, since the source of the $f_{M\pm}$ is located at $s = 0$, we require that

all trajectories of $f_{M\pm}$ be accessible to $s = 0$ by the criterion discussed in the previous section, i.e., that $v_{\parallel 0}^2 > 0$. Noting that magnetospheric particles may be anisotropic, we postulate an otherwise bi-Maxwellian form for $f_{M\pm}$ at the equator, so that

$$f_{Mq}(v_{\parallel s}, v_{\perp s}, V_s) = C_{Mq} [\theta(-v_{\parallel \ell}^2) + \theta(v_{\parallel s})\theta(v_{\parallel \ell}^2)]\theta(v_{\parallel 0}^2) \\ \times \exp \left\{ - (m_q v_{\parallel s}^2 / 2\kappa T_{\parallel q}) - (q|e|V_s / \kappa T_{\parallel q}) \right. \\ \left. - (m_q v_{\perp s}^2 / 2\kappa T_{\perp q}) [1 - (B_0/B_s)] - (m_q v_{\perp s}^2 / 2\kappa T_{\perp q}) (B_0/B_s) \right\}, \quad (9)$$

where κ is the Boltzmann constant and C_{Mq} is a normalization constant defined in such a way that the equatorial number density is given by

$$N_{Mq} = 2\pi \int_{-\infty}^{+\infty} dv_{\parallel} \int_0^{\infty} v_{\perp} dv_{\perp} f_{Mq}(v_{\parallel}, v_{\perp}; 0^+). \quad (10)$$

The unit step function $\theta(x)$ is defined as $+1$ for $x \geq 0$ and vanishes for $x < 0$.

For ionospheric electrons, we require accessibility from the source at $s = \ell$, i.e., we require that $v_{\parallel \ell}^2 > 0$. The condition $v_{\parallel 0}^2 \gtrless 0$ distinguishes between electrons that mirror before reaching the equator ($v_{\parallel 0}^2 < 0$) and those that cross the equator ($v_{\parallel 0}^2 > 0$) to be lost in the conjugate ionosphere. However, the "loss cone" is assumed to be completely filled in either case, and the distribution function is not complicated by this distinction. All cold electrons that enter the ionosphere are assumed to be

replenished immediately and the ionosphere is considered completely symmetrical between north and south. Thus, we postulate an ionospheric electron distribution function, which is taken to be an isotropic Maxwellian distribution of temperature T_{I-} , at $s = \ell$:

$$f_{I-}(v_{\parallel s}, v_{\perp s}; V_s) = (m_- / 2\pi\kappa T_{I-})^{3/2} N_{I-} \theta(v_{\parallel \ell}^2) \times \exp \left\{ - (m_- v_s^2 / 2\kappa T_{I-}) - (q|e| / \kappa T_{I-})(V_s - V_\ell) \right\}, \quad (11)$$

where N_{I-} is the cold ionospheric electron density at $s = \ell$.

For cold ions, the effect of gravity must be taken into account.

Thus, the mapping relationship between the source point $(v_{\parallel \ell}, v_{\perp \ell}; \ell)$ and the point $(v_{\parallel s}, v_{\perp s}; s)$, analogous to (6), is

$$v_{\parallel \ell}^2 = v_{\parallel s}^2 + [1 - (B_\ell / B_s)] v_{\perp s}^2 + (2|e| / m_q)(V_s - V_\ell) + 2GM_E [(1/r_\ell) - (1/r_s)], \quad (12)$$

where G is the gravitational constant, M_E is the mass of the earth, and r_s is the radial distance between the center of the earth and the point s . The quantity $GM_E m_{O+} / R_E$ is approximately 10.53 eV; therefore, the influence of gravity upon the distributions of cold ion-density and parallel electrostatic potential is important near the foot of the field line, where $|e|(V_\ell - V_s)$ is of comparable magnitude.

The dominant ionic species in the topside ionosphere are O^+ and H^+ . The mass difference between the two species influences their relative distributions along the field line and creates an additional charge-separation electric field, as in the polar wind (Banks and Holzer, 1968), although we are dealing with closed field lines. While such an effect may be important in connection with the distribution of O^+ and H^+ ions at the foot of the field line, we note again that such a charge-separation electric potential is orders of magnitude smaller than V_ℓ , which is of the order of kilovolts. Thus, for the sake of simplicity in exposing what are possibly the major factors in the maintenance of V_ℓ , we assume that the ionosphere consists of H^+ ions only. A treatment of the mutual consistency between the large auroral parallel electrostatic potential and the distributions of O^+ and H^+ ions in the trough region of the ionosphere will be given in subsequent work on the formation of the ionospheric trough. For the present paper, we use the cold ion distribution

$$\begin{aligned}
 f_{I+}(v_{\parallel s}, v_{\perp s}; V_s) &= (m_+/2\pi\kappa T_{I+})^{3/2} N_{I+} \theta(v_{\parallel \ell}^2) \theta(-v_{\parallel s}) \\
 &\times \exp \left\{ - (m_+ v_s^2 / 2\kappa T_{I+}) - (|e|/\kappa T_{I+})(V_s - V_\ell) \right. \\
 &\quad \left. - (GM_E m_+ / \kappa T_{I+}) [(1/r_\ell) - (1/r_s)] \right\}, \quad (13a)
 \end{aligned}$$

which is the mapping of a simple Maxwellian distribution in accordance with (12). This distribution is similar to that postulated by Lemaire and

Scherer (1973): we assume that upward-moving ions are lost as they cross the equator so that there are no downward-moving ions in the interval $0 < s \leq \ell$.

For the sake of completeness, we have also experimented with forms for which the ion stream has speed $u (>0)$ at $s = \ell$, as in the polar wind:

$$f_{I+}(v_{\parallel s}, v_{\perp s}; V_s) = (m_+/2\pi\kappa T_{I+}) N_{I+} \theta(-v_{\parallel s}) \delta(v_{\parallel \ell} + u) \\ \times \exp(-m_+ v_{\perp s}^2 B_\ell / 2\kappa T_{I+} B_s), \quad (13b)$$

and

$$f_{I+}(v_{\parallel s}, v_{\perp s}; V_s) = (m_+/4\pi\kappa T_{I+}) N_{I+} \exp(-m_+ v_{\perp s}^2 B_\ell / 2\kappa T_{I+} B_s) \\ \times [\delta(v_{\parallel \ell} + u) \theta(-v_{\parallel s}) + \delta(v_{\parallel \ell} - u) \theta(v_{\parallel s})]. \quad (13c)$$

The form (13b) resembles (13a) and that used by Lemaire and Scherer (1973) in that upward-moving ions are considered to be lost as they cross the equator. The form given by (13c) resembles that postulated by Schulz and Koons (1972) in that it consists of two oppositely directed streams at all points along the field line. The mapping of (13b) and (13c) is in accordance with (12); therefore, we have to make sure that the ion stream will be accessible to $s = \ell$. We have shown that ions are not trapped (so as to be inaccessible to both $s = 0$ and $s = \ell$) by the combined electrostatic and gravitational potential if V_s varies sufficiently with B_s near the foot of the field line. In a proper treatment, utilizing the form (13a) for the O^+ and H^+ species separately, the artificial modeling of an upward flow at the foot of the field line is unnecessary.

In the construction of ion distributions above, we have ignored the important effect of the magnetospheric convection electric field upon the cold ions in the auroral flux tube. Under the action of the perpendicular convection electric field, the particles begin to drift across \vec{B} . Electron drift is negligible on the bounce time scale, but cold-ion drift is not. The net result is a loss of cold ions from the flux tube. Whereas Lemaire and Scherer (1973) postulated the loss process to have occurred entirely at the equator, we have attempted to model the depletion of ions along the flux tube by assuming that the convection electric field causes a constant probability of cold-ion depletion per unit field-line length. Thus, the distributions (13) are to be multiplied by a depletion factor

$$D = \exp \left\{ - \int_s^{s_f} \frac{ds'}{\tau} \frac{[\theta(-v_{\parallel s'}) - \theta(v_{\parallel s'})]}{|v_{\parallel s'}|} - 2 \int_0^{s_f} \frac{ds'}{\tau} \frac{\theta(v_{\parallel s'})}{|v_{\parallel s'}|} \right\}, \quad (14)$$

where τ , the time constant for the process, need not be very long in comparison with the cold-ion bounce period. In the present model, we assume τ to be an adjustable parameter, and τ is generally found to be of the order of 20 minutes. Since the inclusion of (14) in the distribution function (13) of cold ions renders the density moment integrations entirely intractable, we assume $v_{\parallel s'}$ in (14) to be given by the parallel velocity of a cold ion stream free of the influence of the magnetic field, i. e., by

$$v_{\parallel s'} = \left\{ u^2 + (2|e|/m_+)(V_\ell - V_{s'}) + 2GM_E \left[(1/r_{s'}) - (1/r_\ell) \right] \right\}^{1/2}, \quad (15)$$

where u , assumed to be approximately one half of the cold-ion thermal speed, is the upward flow speed at the foot of the field line. With the use of a trial model of $V_{s'}$, the depletion factor D is thus made independent of the phase-space integrations and the cold-ion density is given by the product of the density moment obtained from (13a) and the depletion factor D .

Backscattered electrons are assumed to be produced at altitudes below $s = \ell$ in a manner that yields isotropic distributions at $s = \ell$, but $s = \ell$ is regarded as the source of backscattered electrons in the sense that accessibility to $s = s^*$ requires $v_{\parallel \ell}^2 > 0$. As in the model of Evans (1974), which is based on the abstracted results of a detailed calculation by Banks et al. (1974), we distinguish two populations of backscattered electrons: the primary backscattered electron distribution $f_{S1}(v_{\parallel s}, v_{\perp s}; V_s)$ and the secondary distribution $f_{S2}(v_{\parallel s}, v_{\perp s}; V_s)$. Both distributions of backscattered electrons are related to the precipitating magnetospheric electron flux per unit kinetic energy ϵ_ℓ at $s = \ell$, namely

$$\begin{aligned}
dJ_{M\downarrow}/d\epsilon_\ell &= 2\pi \int_0^1 (2\epsilon_\ell/m_-^2) \cos \alpha_\ell f_{M-}(v_{\parallel\ell}, v_{\perp\ell}; V_\ell) \theta(v_{\parallel\ell}^2) d(\cos \alpha_\ell) \\
&\approx 2\pi (\epsilon_\ell/m_-^2) C_{M-} \theta(\epsilon_\ell - |e|V_\ell) \\
&\quad \times \exp[- (\epsilon_\ell/\kappa T_{\parallel-}) + (|e|V_\ell/\kappa T_{\parallel-})] .
\end{aligned} \tag{16}$$

We estimate the relationship between the upward primary backscatter flux $dJ_{S1\uparrow}/d\epsilon_\ell$ and the total precipitating flux $dJ_\downarrow/d\epsilon_\ell$ of energetic electrons by means of a transfer function $S(\epsilon_\ell, \epsilon'_\ell)$ in the integral equation

$$dJ_{S1\uparrow}/d\epsilon_\ell \equiv \int_0^\infty S(\epsilon_\ell, \epsilon'_\ell) (dJ_\downarrow/d\epsilon'_\ell) d\epsilon'_\ell . \tag{17}$$

The total precipitating flux $dJ_\downarrow/d\epsilon'_\ell$ in (17) is given by the sum of the magnetospheric precipitating flux, $dJ_{M\downarrow}/d\epsilon'_\ell$ in (16), and the precipitating flux of the primary backscattered electrons, $dJ_{S1\downarrow}/d\epsilon'_\ell$. Kinematical considerations require that $J_{S1\downarrow} = J_{S1\uparrow}$, since the discussion on thermal electrons applies equally well to backscattered electrons: whatever goes up must come down. For the primary-backscatter transfer function $S(\epsilon_\ell, \epsilon'_\ell)$, we choose a form given by

$$S(\epsilon_\ell, \epsilon'_\ell) = [\epsilon_\ell/(\epsilon'_\ell)^2] \theta(\epsilon'_\ell - \epsilon_\ell) . \tag{18}$$

This represents an analytically convenient fit to the transfer function deduced by Evans (1974) from a detailed calculation by Banks et al. (1974). The normalization of (18) yields an integrated probability of 0.5 for an incident electron to be backscattered with energy ϵ_l between 0 and ϵ_l' . This agrees well with the estimate by Evans (1974) that 46% of the incident electron flux is backscattered. Thus, we obtain the relationship

$$dJ_{S1\uparrow}/d\epsilon_l = \int_{\epsilon_l}^{\infty} [\epsilon_l/(\epsilon_l')^2] [(dJ_{M\downarrow}/d\epsilon_l') + (dJ_{S1\uparrow}/d\epsilon_l')] d\epsilon_l' , \quad (19)$$

where we have expressed $J_{\downarrow} = J_{M\downarrow} + J_{S1\downarrow} = J_{M\downarrow} + J_{S1\uparrow}$. The solution of (19) for $dJ_{S1\uparrow}/d\epsilon_l$ in terms of $dJ_{M\downarrow}/d\epsilon_l$ is effected by multiplication of both sides by $1/\epsilon_l$ and differentiation with respect to ϵ_l . These steps yield

$$\frac{1}{\epsilon_l} \frac{d}{d\epsilon_l} \left[\frac{dJ_{S1\uparrow}}{d\epsilon_l} \right] = - \frac{1}{\epsilon_l^2} \frac{dJ_{M\downarrow}}{d\epsilon_l} \quad (20)$$

The solution of (20) is given by

$$dJ_{S1\uparrow}/d\epsilon_l = \int_{\epsilon_l}^{\infty} (d\epsilon_l'/\epsilon_l') (dJ_{M\downarrow}/d\epsilon_l')$$

$$\approx (2\pi\kappa T_{\parallel-}/m_-^2) C_{M-} \{ \theta(|e|V_L - \epsilon_L) + \theta(\epsilon_L - |e|V_L) \exp[(|e|V_L - \epsilon_L)/\kappa T_{\parallel-}] \} \quad (21)$$

upon insertion of (16) above. The integration of (16) and (21) with respect to ϵ_L reveals a total precipitation flux

$$\begin{aligned} J_{\downarrow} &\equiv J_{M\downarrow} + J_{S1\downarrow} \approx 2J_{M\downarrow} \approx 2J_{S1\downarrow} \\ &\approx 4\pi(\kappa T_{\parallel-}/m_-)^2 C_{M-} [1 + (|e|V_L/\kappa T_{\parallel-})] . \end{aligned} \quad (22)$$

Thus, we find that half of the precipitating energetic electron flux is magnetospheric, while the other half consists of electrons previously backscattered.

The secondary backscatter is characterized (Banks et al., 1974; Evans, 1974) by a "universal" spectrum having an intensity proportional to the total flux J_{\downarrow} of incident energetic electrons. The secondary flux is negligible ($\leq 1\%$ of maximum) at energies $\epsilon_L \geq 200$ eV, and so we obtain a fit in simple analytic form of the lower-energy portion of the "universal" secondary backscatter spectrum given by Banks et al. (1974):

$$dJ_{S2\uparrow}/d\epsilon_L \approx (\epsilon_L/\epsilon_2^2) A_2 [1 + (\epsilon_L/\epsilon_2)]^{-4} J_{\downarrow} , \quad (23)$$

where $A_2 \approx 3.0$, $\epsilon_2 \approx 15$ eV, and J_{\perp} is given by (22). In the application of the present model to various observations to be considered in the next section, we found it necessary to vary A_2 somewhat in order to fit the low-energy portions of observed electron spectra; therefore, A_2 will be considered an adjustable parameter of the model.

It remains necessary to convert the upward differential fluxes given by (21) and (23) into distribution functions $f_{Si}(v_{\parallel s}, v_{\perp s}; V_s)$, where $i = 1, 2$. We do this by assuming that the backscatter distributions are isotropic (cf. Banks et al., 1974; Evans, 1974) at $s = \ell$. One then obtains the relationship

$$dJ_{Si}/d\epsilon_{\ell} = (2\pi\epsilon_{\ell}/m_{\perp}^2) f_{Si}(v_{\ell}; V_{\ell}) \quad , \quad (24)$$

from which we derive the following backscattered electron distribution functions:

$$\begin{aligned} f_{Si}(v_{\parallel s}, v_{\perp s}; V_s) &\approx (2\kappa T_{\parallel -}/m_{\perp}) C_{M-} \theta(v_{\parallel \ell}^2) \{ \theta(2|e|V_{\ell} - m_{\perp} v_s^2) \\ &+ \theta(m_{\perp} v_s^2 - 2|e|V_{\ell}) \exp[(2|e|V_s - m_{\perp} v_s^2)/2\kappa T_{\parallel -}] \} \\ &\div [v_s^2 + (2|e|/m_{\perp})(V_{\ell} - V_s)] \quad (25) \end{aligned}$$

and

$$f_{S2}(v_{\parallel s}, v_{\perp s}; V_s) \approx 2(\kappa T_{\parallel -} / \epsilon_2)^2 C_{M-} A_2 [1 + (|e| V_{\perp} / \kappa T_{\parallel -})] \theta(v_{\parallel}^2) \div [1 + (|e| / \epsilon_2)(V_{\perp} - V_s) + (m_- v_s^2 / 2\epsilon_2)]^4 \quad (26)$$

For electrons on trapped trajectories, we construct their distribution $f_T(v_{\parallel s}, v_{\perp s}; V_s)$ by assuming it to be a Maxwellian distribution in equilibrium with the "source", from which the trapped electrons had been scattered onto their present trajectories (Lemaire and Scherer, 1971b). In our model, there are two such possible "sources", namely those at $s = 0$ and at $s = \ell$. Thus, for each "source" j , we construct a trapped electron distribution

$$f_{Tj}(v_{\parallel s}, v_{\perp s}; V_s) = (m_- / 2\pi\kappa T_j)^{3/2} N_j(s_j^*) \theta(-v_{\parallel 0}^2) \theta(-v_{\parallel \ell}^2) \times \exp \left\{ - (m_- v_s^2 / 2\kappa T_j) + (|e| / \kappa T_j)(V_s - V_{s_j^*}) \right\}, \quad (27)$$

where s_j^* is the location of the "source" and T_j is an adjustable temperature for the trapped population. For $j = 1$, we identify f_{T1} with the distribution scattered into trapped trajectories from f_{M-} , and so we take $N_1(s_1^*) = N_{M-}$. For $j = 2$ we identify f_{T2} with the distribution of electrons that have been scattered into trapped trajectories from distributions whose sources are at $s = \ell$. There are several such "source"

distributions, but calculations reveal that the density moments of low-temperature trapped particles originally injected at $s = \ell$ are negligible due to phase-space limitations if $V_\ell \sim 1$ kilovolt. Therefore, we identify f_{T2} with electrons scattered into trapped trajectories from f_{S1} . Since the primary backscattered electron distribution has temperature $T_{\parallel -}$, we assume both trapped distributions to have the same temperature $T \equiv T_{\parallel -}$, forming a single distribution

$$f_T(v_{\parallel s}, v_{\perp s}; V_s) = (m_- / 2\pi\kappa T)^{3/2} N_T \theta(-v_{\parallel 0}^2) \theta(-v_{\parallel \ell}^2) \\ \times \exp \left[- (m_- v_s^2 / 2\kappa T) + (|e| V_s / \kappa T) \right], \quad (28)$$

where

$$N_T = N_{M-} + N_{S1} \exp(-|e| V_\ell / \kappa T), \quad (29)$$

N_{S1} being the density derived from f_{S1} at $s = \ell$. The existence of trapped electrons had been assumed in previous exospheric models of the solar wind (Lemaire and Scherer, 1971b), but not in the magnetosphere (Eviatar et al., 1964; Lemaire and Scherer, 1973). Observational evidence for or against their existence would be welcome. Perhaps one may argue that certain regions of phase space would be empty if trapped electrons do not exist (see Figure 1b). Evidence suggesting the filling of all regions of phase space in auroral electron-precipitation events is given by Kaufmann et al. (1976).

Figure 1 summarizes the regions of phase space occupied by the various particle populations discussed above. The left panel indicates velocity-space demarcations that characterize the various portions of the magnetospheric and ionospheric populations of ions. The right panel illustrates the corresponding velocity-space demarcations for electrons.

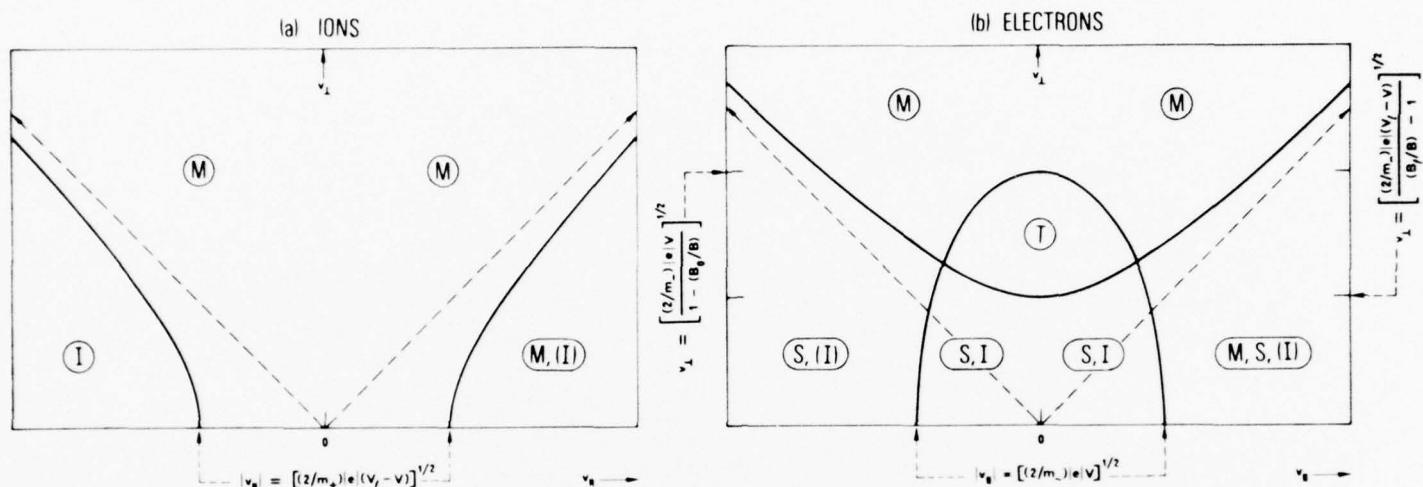


Figure 1. The regions of phase space occupied by the various particle populations are shown schematically for (a) ions and for (b) electrons. The solid curves are demarcations in phase space for the various populations of particles identified by labels in circles or in cartouches: M for particles of magnetospheric origin, I for particles of ionospheric origin, S for backscattered electrons, and T for electrons trapped between mirror points that both lie on the same half of the field line. The ionic label I in parentheses refers to the population given by (13c), as distinguished from those given in (13a) and (13b). The electronic labels I in parentheses indicate phase space regions occupied by electrons in the extreme tail of the cold ionospheric energy distribution. The dashed diagonal lines are the asymptotes $v_{\parallel} = \pm [(B_{\ell}/B) - 1]^{1/2} v_{\perp}$ of the hyperbolic phase space demarcations between $v_{\parallel}^2 > 0$ and $v_{\parallel}^2 < 0$.

THE MODEL

In the previous two sections we have summarized the manner in which charge neutrality is to be enforced on the constructed particle distributions in an auroral flux tube. The general features of the model dealt with in the previous sections are quite akin to those of the exosphere and plasma-sheet models of Lemaire and Scherer (1971b, 1973, 1977), although considerations such as accessibility of sources, anisotropy of magnetospheric particles, and the inclusion of backscattered electrons characterize the greater generality of the present formulation. However, it is mainly the area of model usage which distinguishes the present model from previous exospheric models, since the major purpose of the present model is to explore the factors that may contribute to the maintenance of a large auroral potential difference between the equator and the ionosphere. Therefore, we apply our model to specific electron-precipitation events for which distinctly beam-like energetic electrons are observed.

A second feature involving the usage of our model has to do with the geometry of the assumed magnetic field. In the construction of particle distributions in the previous section, we have tacitly assumed that the model is to be applied to particle and electric-field distributions in a closed dipolar flux tube. While we shall continue to assume so in the rest of this work, we wish to note that the physical processes discussed in this work are also applicable to regions of open field lines. For regions of open field lines, it would be necessary to reconstruct

the particle distributions discussed in the previous section. Although magnetospheric particles in such open-field-line regions are likely to be isotropic, a large electrostatic potential difference may still be maintained by virtue of electron backscatter. Applications of our model of particle and electric field distributions for open field-line regions will be considered in a subsequent work.

In typical observations, either the electron flux distribution (at a given pitch angle) $dJ_-/d\epsilon d\Omega$ or the electron energy flux (at a given pitch angle) $\epsilon dJ_-/d\epsilon d\Omega$ is observed at an altitude below 2000 km. As a first step in the usage of our model, we require that the theoretical flux distribution at the foot of the field line, i.e.,

$$(dJ_-/d\epsilon d\Omega) = (2\epsilon/m_-^2) [f_{M_-}(\epsilon, \alpha; V_\ell) + f_{S1}(\epsilon, \alpha; V_\ell) + f_{S2}(\epsilon, \alpha; V_\ell) + f_{L_-}(\epsilon, \alpha; V_\ell)], \quad (30)$$

where α is the pitch angle and $d\Omega$ the corresponding element of solid angle, be fitted to the observed flux distribution. Except for events in which diffusive energy gain is evident (Evans, 1975), good fits are usually obtained. The parameters V_ℓ , $T_{\parallel -}$, (N_{M_-}/T_{L_-}) , and A_2 are stringently constrained by the fitting. Specific examples of fits to observed particle-flux and observed energy-flux distributions are shown in Figures 2 and 3, respectively. Detailed discussions of the cases will be given in the next section. In the usual situation, only the electron-flux distribution

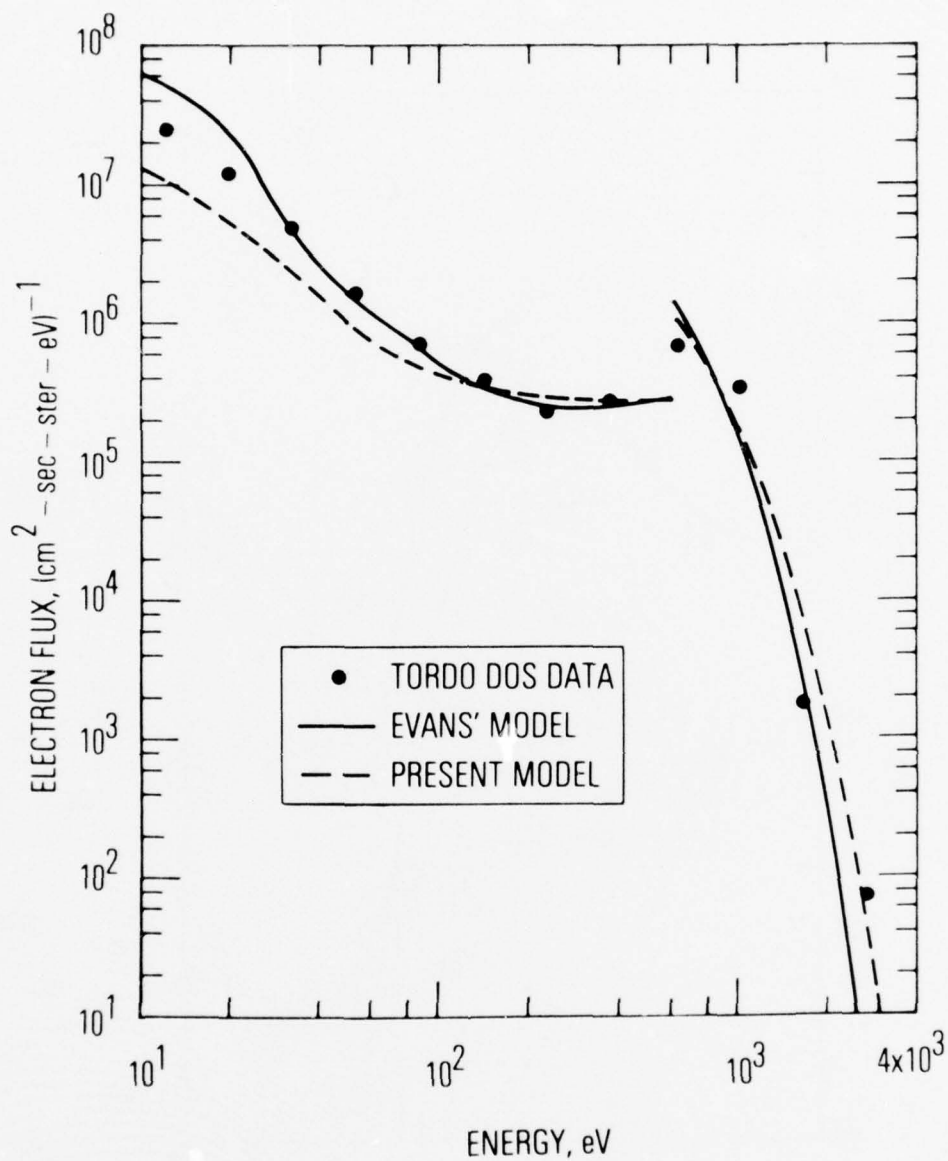


Figure 2. Electron flux at 45° pitch angle observed in the day-side cusp region on 11 January 1975 on board the Tordo Dos rocket (Winningham *et al.*, 1977) is shown as function of electron energy. The data points and the fit (solid curve) corresponding to Evans' model are taken from Evans (1974).

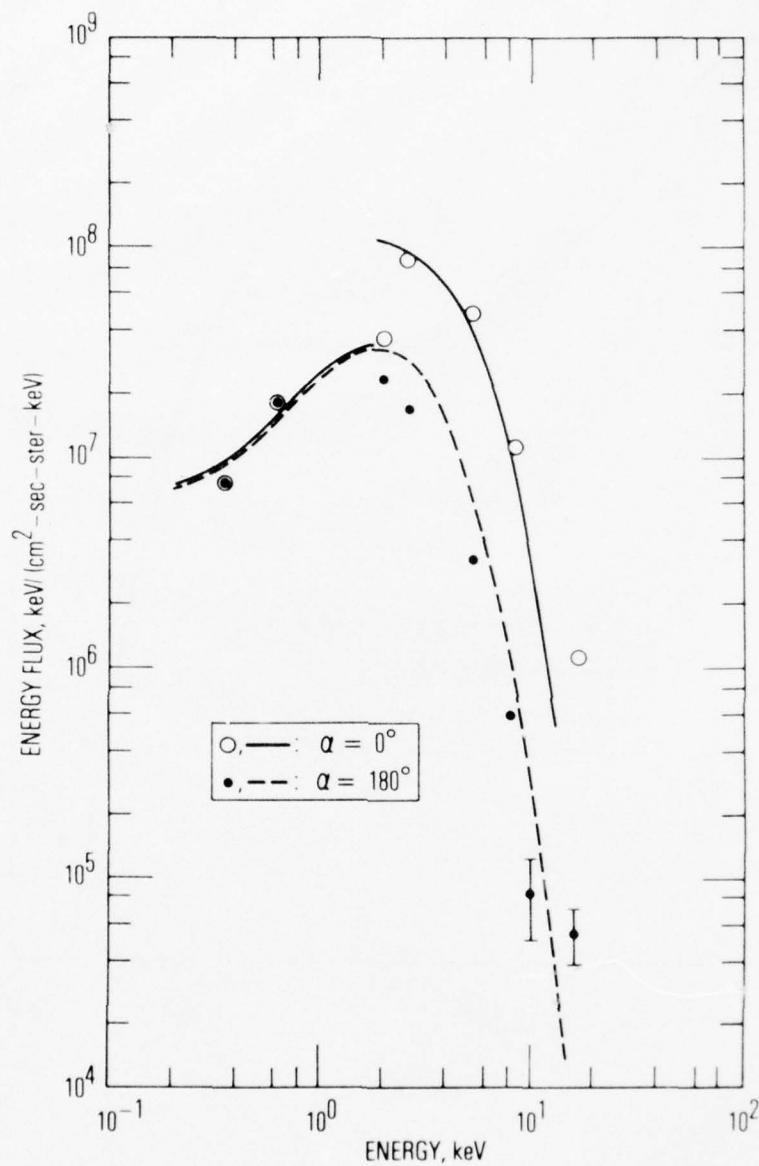


Figure 3. Electron energy fluxes at 0° and at 180° pitch angles observed in an "inverted-V" structure (Mizera *et al.*, 1976) are shown as functions of electron energy. The difference between the downgoing and upgoing fluxes at 1.76 keV indicates the presence of a "monoenergetic" beam of precipitating energetic electrons.

for a specific event is available for comparison with the theoretical flux; therefore, we assume the ion parameters to be variable in the search for a self-consistent parallel electrostatic potential V_s . Should energetic ion distributions be available, a self-consistency check of our model can be made immediately since V_ℓ is a common parameter for both electron and ion distributions. In the usage of our model, the field-aligned current

$$J_{\parallel} \equiv |e| \int_0^{\infty} v_{\perp s} dv_{\perp s} \int_{-\infty}^{+\infty} [f_+(v_{\parallel s}, v_{\perp s}; V_s) - f_-(v_{\parallel s}, v_{\perp s}; V_s)] v_{\parallel s} dv_{\parallel s} \quad (31)$$

is neither made to vanish nor assigned any particular numerical value, as is done in Lemaire and Scherer (1973). If J_{\parallel} is measured for a specific event to which we apply our model, then an additional consistency check can be made on the model since V_ℓ is again a common parameter in (30) and (31). In general, because of the assumed magnetospheric particle anisotropy, and because of the loss of cold ions to the magnetospheric convection pattern, J_{\parallel} is nonvanishing in our model. Further, the loss of cold ions from the flux tube implies that a perpendicular current J_{\perp} also exists. Such considerations raise the question of how to complete the electrical circuit in the auroral region. This presumably occurs via other field lines than the one under consideration and presumably involves perpendicular electric fields which co-exist with the parallel electric field. It is not our intention to explore here the mechanisms by which

any such magnetospheric circuits are closed. In subsequent work, such questions will be addressed in connection with the so-called "inverted-V" structures.

Having obtained the parameters V_ℓ , $T_{\parallel-}$, (N_{M-}/T_{I-}) and A_2 from a comparison of (28) with data for a specific event, we next proceed to implement the quasi-neutrality condition (1). Since we have assumed specific forms for the distribution functions, we calculate the density moments of $f_{M\pm}$, $f_{I\pm}$, f_{Si} and f_T (in closed form) as functions of V_s , B_s , and the particle parameters ($N_{M\pm}$, $N_{I\pm}$, $T_{\parallel\pm}$, $T_{I\pm}$, T , A_2 , and τ). Examples of the required velocity-space integrations, some of which are quite tedious, are given in Appendix B. Not all of the above particle parameters are entirely independent, since the limits of (1) as $s \rightarrow 0$ and as $s \rightarrow \ell$ constitute two constraints among the above particle parameters and the potential difference V_ℓ . Thus, only the parameters N_{I+} , $T_{\parallel+}$, T_{I+} , T_{I-} , T , and τ may be considered free parameters of the model, although the known conditions of the ionosphere in the auroral region impose additional bounds on N_{I+} and $T_{I\pm}$. A summary of the parameters of the model is given in Table 1.

Once the particle parameters are specified, subject to the constraints discussed above, we consider (1), the quasi-neutrality equation in integrated form, as a transcendental equation to be solved for V_s as a function of B_s .

Table 1. Parameters of the Model

| Parameters | Symbols | Remarks |
|--|------------------|---|
| Total Potential Difference | V_ℓ | Determined from observed electron flux |
| Magnetospheric Electron Density at $s = 0$ | N_{M-} | N_{M-}/T_{I-} determined from observed electron flux |
| Magnetospheric Electron Temperatures | T_{I-}, T_{I+} | T_{I-} and N_{M-}/T_{I-} determined from observed electron flux |
| Magnetospheric Ion Density at $s = 0$ | N_{M+} | Determined by charge-neutrality constraint at $s = 0$ |
| Magnetospheric Ion Temperatures | T_{I+}, T_{I+} | Adjustable, constrained by $T_{I+} \geq T_{I+}$ and $T_{I+} \sim 4T_{I-}$ |
| Ionospheric Electron Density | N_{I-} | Determined by charge-neutrality constraint at $s = \ell$ |
| Ionospheric Electron Temperature | T_{I-} | Adjustable, but fixed at $T_{I-} = 1$ eV here; unimportant |
| Ionospheric Ion Density | N_{I+} | Adjustable, but constrained to trough-region densities |
| Ionospheric Ion Temperature | T_{I+} | Adjustable, but fixed at $T_{I-}/32$; unimportant |
| Secondary Backscatter Intensity | A_2 | Determined from observed electron flux |
| Trapped Electron Temperature | T | Adjustable, but fixed at $T = T_{I-}$ |
| Cold Ion Depletion Time Constant | τ | Adjustable, but usually turns out to be ~ 20 min |

This is done on the CDC 7600 computer, since a large number of transcendental functions are involved. The "solution" so obtained is, however, not necessarily the required solution of the model, since an acceptable V_s must be a monotonic function of B_s and it must satisfy (7). If V_s does not satisfy these tests, the particle parameters are adjusted and the solution process is repeated until a satisfactory solution is obtained.

RESULTS

Since the primary purpose of the present model is to determine circumstances under which a large electrostatic potential difference may be maintained along an auroral field line, we have applied the model to a number of specific cases, two of which will be discussed in this section.

Figure 2 shows the unidirectional electron flux at 45° pitch angle for an event observed in the dayside cusp region on 11 January 1975 (Winningham et al., 1977). The electron-flux data have been compared with the model (solid curve) of Evans (1974), and the figure is taken from Evans (1975). The data suggest that a monoenergetic beam of particles at an energy ~ 600 eV may be present in the electron spectrum. Figure 3 shows electron energy-flux data at two pitch angles obtained in an "inverted-V" structure (Mizera et al., 1976). This example is particularly interesting not only because of its occurrence in the auroral region (invariant latitude 69.7°) but also because it clearly shows the beam-like character of precipitating high-energy electrons, as is evidenced by the great difference between the unidirectional energy flux at 0° and that at 180° pitch angles. The parameters which determine the model fits shown in Figure 2 (Case W) and in Figure 3 (Case M) are summarized in Table 2.

Table 2: Parameters of the Fit

| Parameter | Case W (Figure 2) | Case M (Figure 3) |
|-------------|---------------------|-----------------------|
| V_i | 0.59 kV | 1.76 kV |
| N_{M-} | 3 cm^{-3} | 0.6 cm^{-3} |
| $n T_{ -}$ | 0.189 keV | 1.23 keV |
| $n T_{1-}$ | 0.775 keV | 4.67 keV |
| A_2 | 4.8 | 3.2 |

Although the parameters shown in Table 2 are not uniquely determined from the data, the comparison between the present model parameters and those of Evans' model for Case W illustrates some differences between the two models. In Evans' model, the number density of the electron beam was taken to be 0.85 cm^{-3} and the temperature was taken to be 0.143 keV . While his electron temperature, which determines the slope of the flux distribution at energies above $|e|V_\ell$, is approximately the same as our parallel temperature kT_{\parallel} , the electron beam density required in Evans' model is considerably smaller than the N_{M-} of our model, primarily because of the fact that in our model only those magnetospheric electrons that would mirror at $s > \ell$ contribute to the energetic electron flux. Further, because of differences in the pitch-angle distributions of the energetic electrons for the two models, the total flux (integrated over pitch angle) is larger in Evans' model than in ours; hence, the low-energy electron fluxes for the two models are also different. For Case M (Figure 3), the required electrostatic potential difference and the required magnetospheric electron temperatures are considerably higher than in Case W (Figure 2). In many respects, Case M is a more stringent test of the model since the electron energy fluxes at two pitch angles are available. In particular, the low-energy portion of the electron spectrum shown in Figure 3 requires considerably lower secondary backscatter than in Figure 2.

With the use of the parameters determined in Table 2, searches for self-consistent electrostatic potentials V_g were made in accordance with the formulation given in the previous two sections. In the solution process,

the model parameters not yet determined in Table 2 are varied in the manner described in Table 1. For Case M, the L value of the field line is 8.35. For Case W, the observations were made at very high invariant latitudes (77.5° N) where the rocket was possibly on open field lines in the cusp region. In this respect, our model is probably not fully applicable, since we assume the magnetospheric particles to be partially trapped by a dipolar field. However, if the precipitating magnetospheric particles were to have the anisotropies determined in the fitting of Figure 2, the application of the model is not substantially changed even though the solution V_s , as a function of B/B_0 , may not be an accurate description of the "true" potential distribution. Since the requirement of the total potential drop V_ℓ remains the same whether one considers open or closed field lines, we attempted an application of our model to Case W by assuming an L value of 8.54 for this event. For this reason, our results for Case W are rather to be viewed as an illustration of our model than as reconstructions of actual particle and potential distributions. The electrostatic potential solutions of (1) satisfying the accessibility criterion (7) for Cases W and M are shown in Figure 4 (Case W) and Figure 5 (Case M) respectively. In Figure 4, it is seen that the potential distribution V_s is concave downward when plotted against the magnetic-field ratio B/B_0 . In Figure 5, the potential distribution V_s is also concave downward although it may not appear so because the magnetic-field ratio is plotted on a logarithmic scale. For Case W (Figure 4), the major part of the potential drop is confined to the region above ~ 10000 km altitude, with parallel electric field intensities

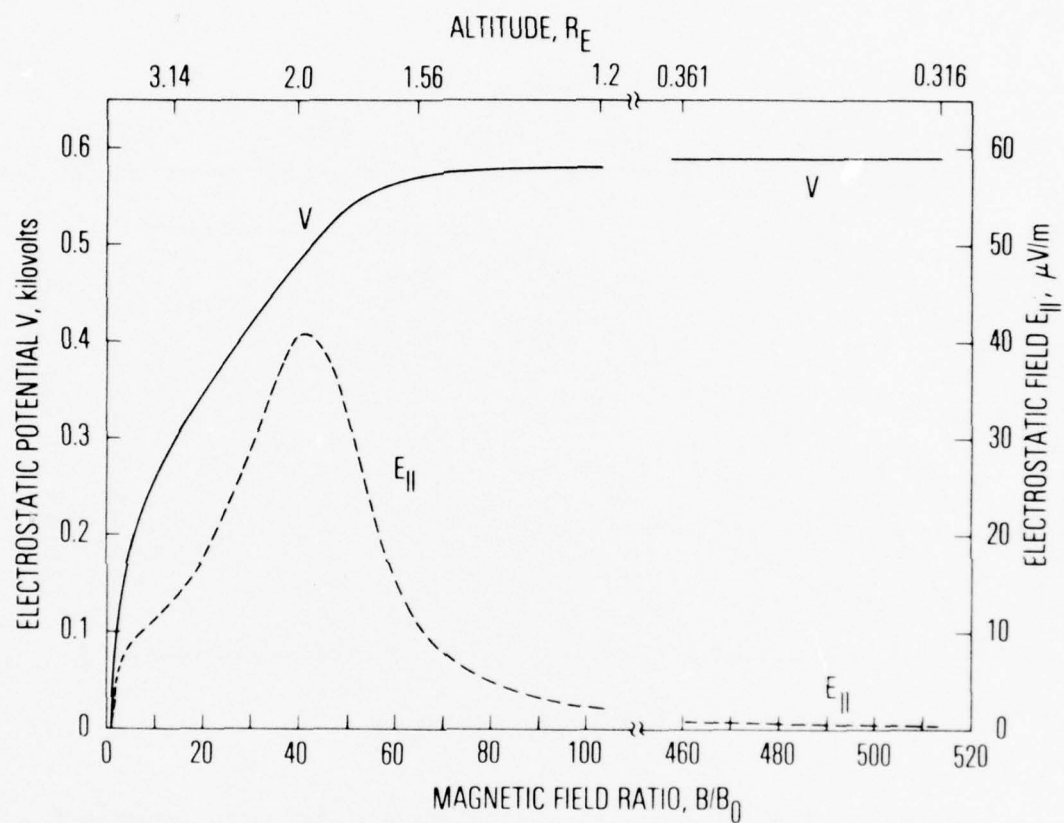


Figure 4. The self-consistent electrostatic potential computed for the case corresponding to the observed electron flux of Figure 2 (Case W) is shown as function of magnetic-field ratio and altitude. The magnitude of the parallel electrostatic field is also shown.

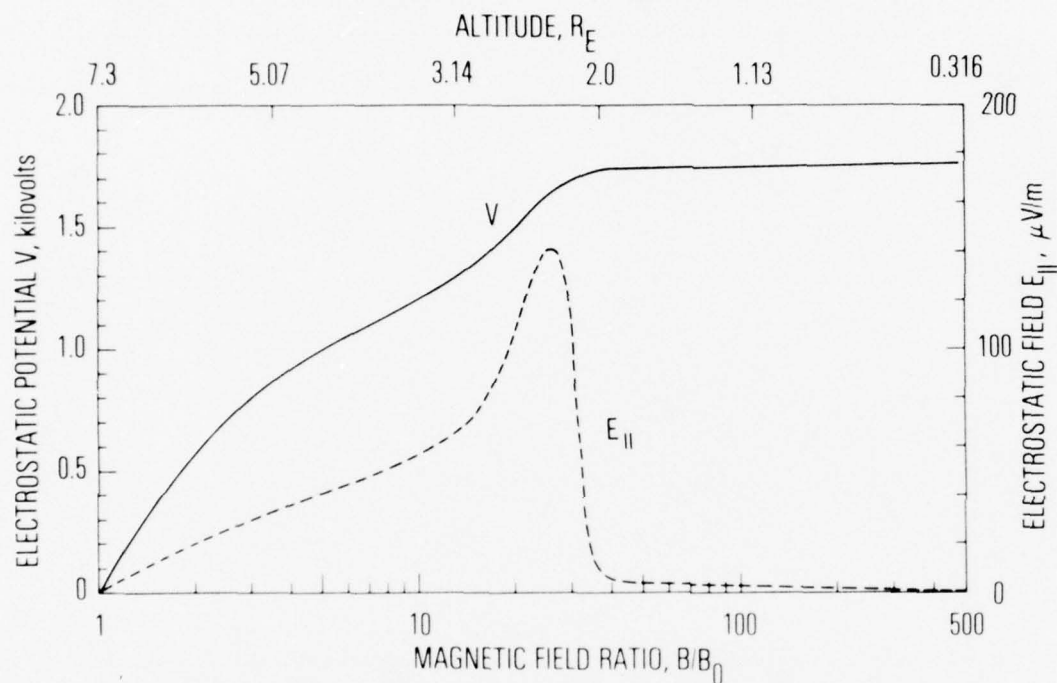


Figure 5. The self-consistent electrostatic potential computed for the case corresponding to the observed electron flux of Figure 3 (Case M) is shown as function of magnetic-field ratio and altitude. The curve for the potential V has the same property of downward concavity as that shown in Figure 4. The difference in appearance between this figure and Figure 4 is due to the logarithmic scale used in plotting the magnetic-field ratio here. The magnitude of the parallel electrostatic field computed for this case is considerably larger than that of Figure 4.

of up to $40 \mu\text{V/m}$. The potential difference V_ℓ for Case M is considerably larger than that for Case W, hence, the parallel electric field intensity in Figure 5 (up to $140 \mu\text{V/m}$) is considerably larger than that in Figure 4. Quite interestingly, the region of major potential drop (above $\sim 12\,000$ km) in Case M is not drastically different from that in Case W, even though the magnitudes of the potential drops are quite different. The self-consistent electrostatic potential distributions for both cases are consistent with Evans' model, where it is assumed that the region of electron acceleration by parallel electric fields is well above the region of electron flux observation. In both cases, the field lines below $10\,000$ km altitude are essentially equipotentials. This common feature may be a weak point in the model, since there is some observational evidence that particle acceleration occurs mainly below the $7\,000$ km altitude (J. F. Fennell and P. F. Mizera, personal communications, 1977). To counterbalance the point, however, there also is some evidence of parallel electric fields above $7\,000$ km from barium-release experiments (Haerendel *et al.*, 1976). Evidently, the observational situation is probably quite variable. On the other hand, the location of intense parallel electric field in our model may be somewhat dependent on the assumed location of the ionospheric boundary. Presumably, if we were able to handle the proper ionospheric boundary condition, which depends on particle species and particle energy, the distribution of V_s might be somewhat different. Moreover, the inclusion of an intense perpendicular electrostatic field in the consideration of charge neutrality would also affect the location of the major parallel

electrostatic potential drop. Evidence for the important influence of very intense perpendicular electric fields upon energetic particle accelerations in the auroral region has recently been reported (Mozer et al., 1977). Perpendicular electrostatic fields, moreover, may play a major role in defining "inverted-V" structures (e.g., Swift, 1975).

The critical model parameters required for the solution of (1), satisfying the accessibility criterion (7), are shown in Table 3. All other model parameters are either fixed or determined by charge-neutrality constraints at $s = 0$ and $s = \ell$, in accordance with the summary in Table 1. Comparison of magnetospheric ion temperatures in Table 3 with magnetospheric electron temperatures in Table 2, for both cases, indicates that the solutions require highly anisotropic electrons ($T_{\perp-}/T_{\parallel-} = 4.1$ for Case W and $T_{\perp-}/T_{\parallel-} = 3.8$ for Case M) and isotropic ions ($T_{\perp+}/T_{\parallel+} = 1$), even though the potential differences and particle densities in the two cases are quite different. Although this peculiar feature, common to both cases, may be a coincidence, we are inclined toward the view that the difference between the pitch-angle anisotropies of electrons and ions required by the model is not accidental. For field lines just poleward of the plasmapause, where the magnetospheric particle populations are probably of ring-current origin, the ion population is susceptible to cyclotron instability at lower pitch-angle anisotropies than the corresponding process for the electrons (Cornwall et al., 1971). Thus, one would expect the equilibrium population to be much more nearly isotropic

Table 3: Parameters Yielding Solutions

| Parameter | Case W (Figure 4) | Case M (Figure 5) |
|-------------------------|------------------------|----------------------|
| N_{I+} | 1200 cm^{-3} | 90 cm^{-3} |
| $\kappa T_{\parallel+}$ | 2.0 keV | 8.0 keV |
| $\kappa T_{\perp+}$ | 2.0 keV | 8.0 keV |
| t | 17 min | 19 min |

for protons than for electrons. For field lines nearer to the cusp, where the magnetic field is very weak, the pitch-angle anisotropy of an ion population is more likely to be destroyed by scattering off magnetic-field inhomogeneities of a given scale size than is the anisotropy of an electron population. Even without consideration of scattering by random magnetic-field inhomogeneities, the motion of ions at a given energy is less likely to be adiabatic than that of electrons at the same energy. Thus, considerations of possible wave-particle interactions and of non-adiabaticity of particle motion in the earth's magnetic field seem to favor a tendency for auroral-zone ions to be more nearly isotropic in pitch-angle distribution than electrons. Such a tendency is consistent with the temperature parameters required for self-consistent solutions in our model.

An important feature of our model concerns the relationship between the magnitude of the parallel potential drop V_ℓ and the ionospheric density N_{I+} required to obtain a self-consistent solution. Comparison of Case W with Case M in Tables 2 and 3 shows that V_ℓ and N_{I+} are inversely related, i. e., to maintain $V_\ell = 0.59$ kV in Case W requires $N_{I+} = 1200 \text{ cm}^{-3}$, whereas to maintain $V_\ell = 1.76$ kV in Case M requires $N_{I+} = 90 \text{ cm}^{-3}$. The sensitivity of our model to the ionospheric density N_{I+} and (in particular) the above inverse relationship are expected, since V_ℓ is essentially maintained by charge separation caused by the difference between magnetospheric particle pitch-angle anisotropies and by the inevitability of electron backscatter. The existence of a parallel potential distribution V_s implies that ions from the ionosphere will be

accelerated up the field line to neutralize the electron excess. Thus, the higher the ion density N_{I+} , the more difficult it is for the model to maintain a large equilibrium potential difference V_ℓ . Although local-time dependence of the ionospheric density is not introduced into the model, the values of N_{I+} required for both cases in Table 3 are consistent with the local time of observation for the two cases. Since Case W was observed in the dayside cusp region and Case M was observed at a local time of 2024 hours, the anticipated day-night difference in ionospheric densities at 2000 km is consistent with the order-of-magnitude difference between N_{I+} for the two cases. It should be noted that N_{I+} was solely determined by the requirement of obtaining a self-consistent solution. The density N_{I+} determined for Case M is consistent with the winter nighttime trough-region ionosphere (Hoffman *et al.*, 1974). The density N_{I+} determined for Case W is also consistent with the winter dayside high-latitude ionosphere, since the event was observed in January 1975 (Winningham *et al.*, 1977). As is discussed above, the maintenance of a kilovolt-magnitude parallel electrostatic potential requires rather low ionospheric densities, which correspond to winter conditions of the polar F-region. Conversely, only very small parallel potential differences may be maintained if the F-region ionospheric densities N_{I+} at 2000 km were $\sim 10^4 \text{ cm}^{-3}$, corresponding to summer daytime conditions. These considerations are applicable only to the general dependence on the ionospheric boundary conditions of our model since the dayside north-south asymmetry

of the ionosphere is neglected in our consideration. Quite interestingly, statistical analysis of OGO-4 data indicated that field-aligned electron precipitation events were more likely to occur during winter (Berko and Hoffman, 1974). Since our model requires ion densities at the lower boundary which are consistent with F-region trough densities only, and further, since energetic O^+ and H^+ ions in the keV range (moving upward along auroral field lines) have been reported (Shelley *et al.*, 1976), we may perhaps invoke the self-consistent parallel electric field as a possible mechanism for the formation of the ionospheric trough. A detailed consideration of such a mechanism will be made in a subsequent work.

The density distributions n_j of particles of various species ($j = M^-$, M^+ , $S1$, $S2$, T , I^- , and I^+) for Case W are shown in Figures 6 and 7. From Figure 6, it is seen that roughly 1/3 of the magnetospheric electrons are precipitating, so as to yield a precipitating electron beam of density 0.9 cm^{-3} , in agreement with the density required in the model of Evans (1975). The density distribution n_{S1} of primary backscattered electrons shows a peculiar kink near the magnetic-field ratio $B/B_0 \approx 300$. The formation of the kink is quite easily understood if one recalls that, according to (21), the primary backscattered electron distribution consists of a low-energy component ($\epsilon_\ell < |e|V_\ell$) and a high-energy component ($\epsilon_\ell > |e|V_\ell$). The high-energy component of primary backscattered electrons has a density distribution similar to n_{M^-} near the foot of the field line, whereas the low-energy component has a distribution similar to the n_{S2} of secondary backscattered electrons,

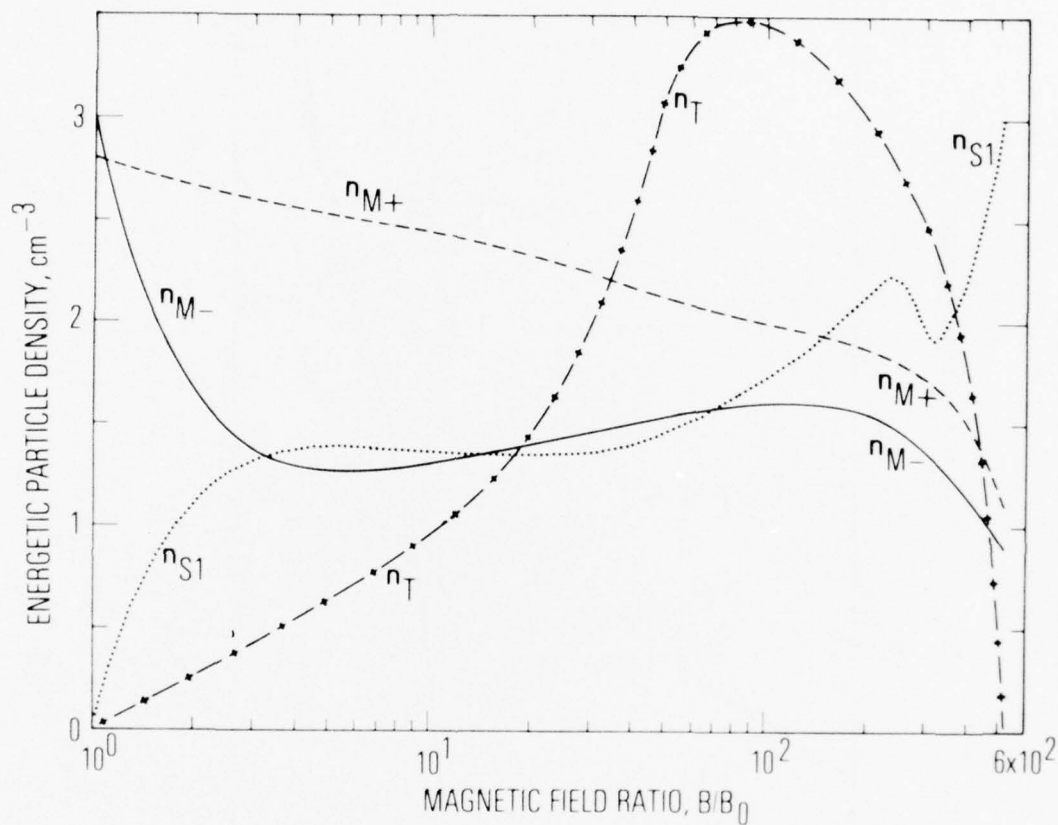


Figure 6. Distributions of the various energetic particles along the field line, computed for Case W, are shown as functions of magnetic-field ratio. The subscripts identify the various particle populations: $M\pm$ for magnetospheric protons and electrons, S1 for primary backscattered electrons, and T for electrons trapped between mirror points that both lie on the same half of the field line.

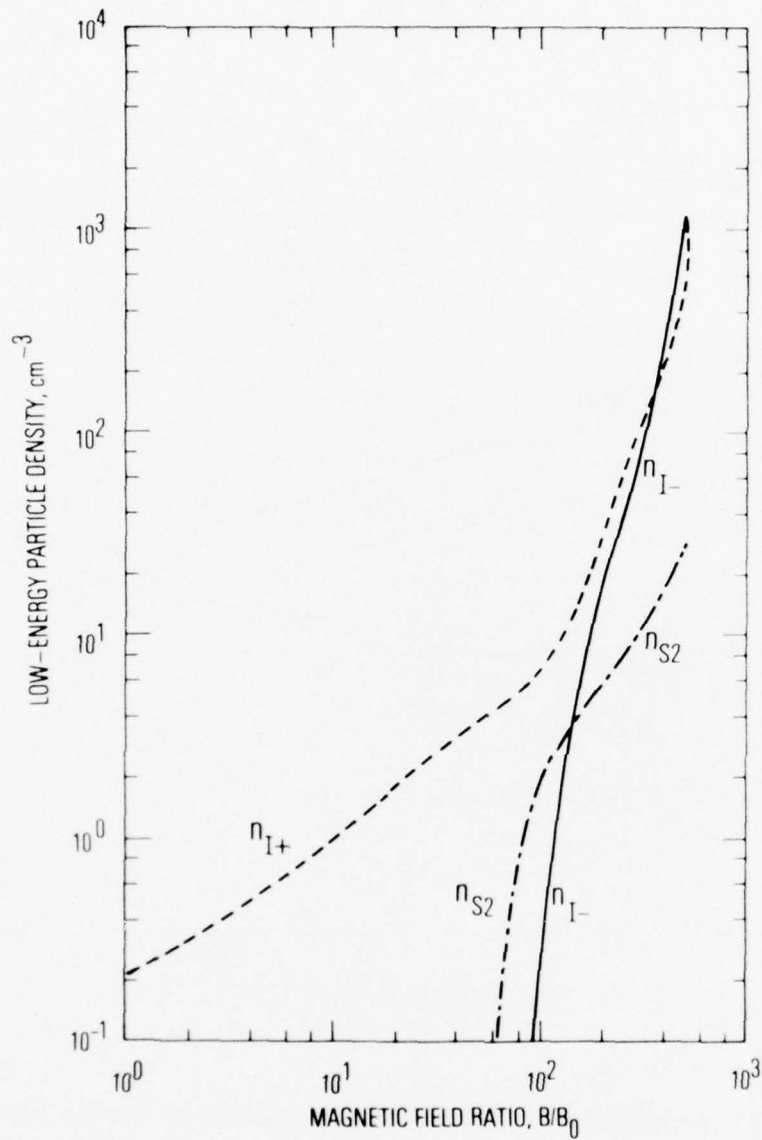


Figure 7. Distributions of the various "low-energy" particles along the field line, computed for Case W, are shown as functions of magnetic-field ratio. The subscripts $I \pm$ refer to ionospheric particles, and the subscript S2 refers to secondary backscattered electrons. At the upper reaches of the field line ($B/B_0 \lesssim 10$) the ions are not truly of low energy since they have been accelerated by the parallel electric field.

shown in Figure 7. The sum of two such curves produces the shape of n_{SI} shown in Figure 6. Comparison of magnetospheric ion density n_{M+} in Figure 6 with ionospheric ion density n_{I+} in Figure 7 in the region just above the intense parallel electric field indicates that the densities of the two species are comparable there. Since the ionospheric ions in this region have been accelerated by the electric field, we would expect substantial numbers of energetic ions in the region, in agreement with Shelley et al. (1976).

CONCLUSION

We have demonstrated in this model that parallel electrostatic potential differences of the order of one kilovolt may be self-consistently maintained along an auroral field line by the magnetospheric and ionospheric particle populations in the flux tube. Our model attempts to abstract the characteristics of magnetospheric and ionospheric particle distributions and to incorporate the very important process of electron backscatter in a magnetic field. By application of the principle of quasi-neutrality, a self-consistent parallel electrostatic potential distribution, in equilibrium with the particle distributions along the auroral field line, is obtained. Application of the model to two typical events of field-aligned electron precipitation have yielded particle parameters which are consistent with the conditions of the ionosphere and the magnetosphere at the time and place of observation of the events. The difference in the pitch-angle anisotropies of magnetospheric ions and electrons and the inclusion of backscattered electrons are the key factors which self-consistently support a parallel potential difference of kilovolt range. Our model suggests that such large parallel potential differences between the ionosphere and the magnetospheric equator can be maintained only if the ion density at the lower boundary (2000 km altitude) is comparable to that in the F-region trough. We are inclined to view the generation of a large parallel electrostatic potential drop as a self-consistent mechanism by which the F-region ionospheric trough is formed by extraction of cold ions from the ionosphere. These cold ions are accelerated upward into the magnetosphere where their energies will be $\sim |e|V_\ell$, i. e., in the keV range.

As we have stated in the introduction, our model is not intended to be applicable to all types of field-aligned electron precipitation events in which beam-like characteristics are evident. In particular, our model is incapable of explaining events in which diffusive energy gain is evident. Further, our model is not intended to exclude the possible existence of double layers or electrostatic shocks. Indeed, it is quite easy to obtain in our model a "solution" which has the characteristics of a double layer similar to that obtained by Lemaire and Scherer (1977). However, such a potential distribution does not satisfy our accessibility criterion imposed by (7). We do not know how to treat the velocity-space integration for particles that are accessible to the source point s^* only under conditions more stringent than the simple criterion on $v_{\parallel}^2 s^*$. Therefore, we are unable to generate "double layer" solutions that are acceptable within the framework of our model.

In a simple model such as ours, there are obviously a number of features which require improvement. Clearly, our assumption of an ionospheric boundary independent of particle species and energy is not justified. The exclusion of perpendicular electric fields in our consideration of quasi-neutrality is clearly not realistic, since auroral events are invariably accompanied by intense perpendicular electric fields (Mozier et al., 1977). We have ignored these crucial features primarily for the sake of simplicity and for the sake of concentrating on the implications of pitch-angle anisotropy, electron backscatter, and ionospheric conditions. We hope to remove these shortcomings of our model in subsequent works.

Finally, we take note of some very recent studies by Lennartsson (1976, 1977) and Whipple (1977), which have some features in common with the present work. We became aware of these studies only after completion of the present numerical calculations, but we do not view the present work as a duplication of their efforts. The problem of calculating parallel electric fields and charged-particle distributions in the auroral zone is a complicated one, and different investigators are likely to approach the problem in somewhat different ways.

APPENDIX A: ACCESSIBILITY

We have used the simple criterion $v_{\parallel s^*}^2 \geq 0$ in order to determine whether a phase-space point $(v_{\parallel s}, v_{\perp s}; s)$ is connected to a source point $(v_{\parallel s^*}, v_{\perp s^*}; s^*)$ under the laws of adiabatic charged-particle motion. Strictly speaking, however, the necessary and sufficient condition for accessibility is that $v_{\parallel s'}^2 > 0$ for all s' between s and s^* . The equivalence of this seemingly more stringent criterion to the simple criterion on $v_{\parallel s^*}^2$ is contingent on the functional form of $V_s(B_s)$, as will be shown here.

We wish to determine some (preferably minimal) constraints on the form of V_s that will assure the truth of the following statement for all particles of interest: if $v_{\parallel s}^2 > 0$ and $v_{\parallel s^*}^2 > 0$, then $v_{\parallel s'}^2 > 0$ for all s' between s and s^* . The statement will obviously hold true if $v_{\parallel s'}^2$ is a monotonic function of $B_{s'}$ for $0 \leq s' \leq \ell$. It will also hold true if $v_{\parallel s'}^2$ is concave downward when plotted as a function of $B_{s'}$ between $s' = 0$ and $s' = \ell$. The presence of $q = \pm 1$ in (12) would make it difficult for both ions and electrons to have a monotonic (or both to have a concave-downward) $v_{\parallel s'}^2$ for all values of $v_{\parallel s}^2$ and $v_{\perp s}^2$. We shall therefore try to make $v_{\parallel s'}^2$ monotonic for ions and concave downward for electrons.

Monotonicity of $v_{\parallel s'}^2$ for ions ($q = +1$) would require that

$$\begin{aligned} d(v_{\parallel s'}^2)/dB_{s'} &= - (v_{\perp s'}^2/B_{s'}) - (2/m_+) |e| (dV_{s'}/dB_{s'}) \\ &+ \frac{4GM_E}{3R_E B_0} \left[\frac{B_0}{B_{s'}} \right]^{2/3} \frac{[4 - 3(r_{s'}/LR_E)]^{5/6}}{[8 - 5(r_{s'}/LR_E)]} \leq 0, \end{aligned} \quad (A1)$$

as can be shown by differentiating (12) with respect to $B_{s'}$, using a centered-dipole model for the magnetic field ($r_{s'} = \text{altitude} + R_E$). The inequality in (A1) is imposed by the leading term, which would dominate in the limit of large v_{1s}^2 . For the same inequality to hold in the limit of small v_{1s}^2 , however, one must have $dV_{s'}/dB_{s'} > 0$ at least. The stronger condition

$$|e| (dV_{s'}/dB_{s'}) > (GM_E m_+ / 3R_E B_0) (B_0/B_{s'})^{2/3} \quad (A2)$$

for $0 \leq s' \leq \ell$ would enable the electric-field term to overcome gravity, as is required for the unconditional monotonicity of $v_{\parallel s'}^2$.

Gravity is negligible for electrons ($q = -1$), but the appearance of $q < 0$ in (6) necessitates a further functional constraint on $V_{s'}$. We require (see above) that $v_{\parallel s'}^2$ for electrons be concave downward when plotted against $B_{s'}$. In other words, we require that

$$d^2(v_{\parallel s'}^2)/dB_{s'}^2 = (2/m_-) |e| (d^2V_{s'}/dB_{s'}^2) \leq 0 \quad (A3)$$

for $0 \leq s' \leq \ell$, which is to say that $V_{s'}$ must be concave downward when plotted against $B_{s'}$.

For electrostatic potentials $V_{s'}$ that fail to satisfy (A2) and (A3), there is a serious danger that a "barrier" in the "effective" potential defined (e.g., Whipple, 1977) by

$$\Phi_{s'} = q |e| V_{s'} + (m_q v_{\perp s'}^2 / 2 B_{s'}) B_{s'} - (m_q G M_E / r_{s'}) \quad (A4)$$

would prevent the access of a particle from s^* to s , despite the fact that both $v_{\parallel s}^2 > 0$ and $v_{\parallel s^*}^2 > 0$ were satisfied for the particle in question. It is to preclude such a danger of improper mapping that we require (A2) and (A3) as constraints (imposed a posteriori) on the admissibility of "solutions" V_s that are found to satisfy (1) for $0 \leq s \leq \ell$.

We have carefully checked to be sure that our solutions $V_s(B_s)$ shown in Figures 4 and 5 satisfy (A3), which is equivalent to (7). We have also verified that our solutions satisfy (A2) for hydrogen ions. However, we find that our solutions fail to satisfy (A2) at $B_s \sim B_\ell$ for heavier ions such as O^+ . This is not a serious drawback in the present context. Since we have considered only one species of ionospheric ion, we may logically identify the I^+ population in (13) with H^+ and consider all the O^+ to reside beyond $s = \ell$, i.e., below the base of collisionless medium. Alternatively, we may regard the I^+ population as consisting of ions having a mass equal to the density-weighted mean of m_H and m_O at $s = \ell$.

Either of the above alternatives can be supported by an appeal to the H^+/O^+ density ratio observed at altitudes below 2000 km in high-latitude trough regions (Hoffman et al., 1974), but neither alternative is

strictly acceptable in the context of accounting for the upward fluxes of energetic O^+ that are observed (Shelley et al., 1976) at high altitudes. We presume that a more realistic treatment of the ionosphere (beyond the scope of the present work) would alleviate this dilemma. Thus, in a more sophisticated study, one might treat the several ionospheric constituents separately and also take account somehow of the smooth transition between the collision-dominated lower ionosphere and the collision-free upper ionosphere. Such a study is in progress.

The only O^+ ions that would have been treated improperly in the present work are some of those found equatorward of the maximum in the effective potential Φ_s , which is defined by (A4). Those found earthward of the maximum in Φ_s would have been mapped in precise accordance with Liouville's theorem, except of course for the depletion factor D given by (14). It is not likely that the more sophisticated treatment of the ionosphere described above will alter the present form of $V_s(B_s)$ severely, so as to let O^+ ions satisfy (A2), for in that case the ionosphere would rapidly be depleted of O^+ . However, a more realistic treatment of the ionosphere would better account for the relative distribution of H^+ and O^+ along the field line and might (by treating the effect of gravity on O^+ in a fully consistent way) enable one to increase the convective sweeping time τ that appears in (14). This would be desirable.

APPENDIX B: DENSITY MOMENT

In this appendix we shall show a sample calculation of the charge-density moment of magnetospheric electrons, which is required for implementing quasi-neutrality. With the use of the distribution function (9) for magnetospheric electrons f_{M-} , we obtain the magnetospheric electron density moment

$$\begin{aligned} n_{M-}(s) &\equiv \int_0^\infty v_{\perp s} dv_{\perp s} \int_{-\infty}^{+\infty} f_{M-}(v_{\parallel s}, v_{\perp s}; V_s) dv_{\parallel s} \\ &\equiv 2\pi C_{M-} (2\kappa T_{\parallel -}/m_-)^{3/2} Q_{M-}(s) \end{aligned} \quad (B1)$$

In our model, the density of magnetospheric electrons $n_{M-}(0)$ at the equator is the input parameter N_{M-} ; therefore, (B1) is normalized so that

$$n_{M-}(s) = N_{M-} [Q_{M-}(s)/Q_{M-}(0)] , \quad (B2)$$

where the function $Q_{M-}(0)$ is defined as the limit of $Q_{M-}(s)$ as $s \rightarrow 0^+$. The function $Q_{M-}(s)$ is given in terms of functions related to error functions and Dawson integrals (Abramowitz and Stegun, 1974). It is convenient to define

$$E_1(x) = \exp(x^2) \int_0^x dy \exp(-y^2) \quad (B3)$$

$$E_2(x) = \exp(x^2) \int_x^\infty dy \exp(-y^2) \quad (B4)$$

$$E_3(x) = \exp(-x^2) \int_0^x dy \exp(y^2) \quad (B5)$$

together with the simplifying relations

$$h_s = B_s - [1 - (T_{\parallel-}/T_{\perp-})] B_0 \quad (B6)$$

$$\lambda_s = (|e| v_s / \kappa T_{\parallel-})^{1/2} \quad (B7)$$

$$\mu_s = [(B_s - B_0) T_{\perp-} / (B_0 T_{\parallel-})]^{1/2} \quad (B8)$$

$$v_s = [(B_{\perp} - B_s) / h_{\perp}]^{1/2} \quad (B9)$$

$$\xi_s = \lambda_s^2 - [(B_s - B_0) / (B_{\perp} - B_0)] \lambda_{\perp}^2. \quad (B10)$$

The function $Q_{M-}(s)$ is given by

$$\begin{aligned}
Q_{M-}(s) = & (B_s/2h_s) \{ (\nu_s \pi^{1/2}/2) \exp[|e| (V_s h_l - V_l h_s)/(B_l - B_s) \kappa T_{||-}] \\
& + E_2(\lambda_s) + \mu_s E_3(\lambda_s/\mu_s) \\
& + \theta(\xi_s) \exp[-(\lambda_l/\mu_l)^2] [\mu_s E_3(\xi_s^{1/2}/\mu_s) - \nu_s E_1(\xi_s^{1/2}/\nu_s)] \} .
\end{aligned}
\tag{B11}$$

The evaluations of the charge densities are independently checked by three methods: (a) the charge-density integrals for the mirroring and precipitating components are evaluated separately and the sum is checked against (B11); (b) if we set $\theta(v_{||s})$ equal to unity in (9), then there are no phase-space restrictions due to the functions $\theta(v_{||l}^2)$ and the total charge-density integral is easy to compute, and we have checked that the total charge-density integral is equal to the sum of the mirroring component plus twice the precipitating component; (c) finally, the arguments of the θ functions in (9) simplify in the limit $s \rightarrow 0^+$, and the evaluation of (B11) in the limit $s \rightarrow 0^+$ has been checked against the $s \rightarrow 0^+$ limit of the charge-density integral independently evaluated before the limit is taken.

REFERENCES

- Abramowitz, M., and I. A. Stegun, Handbook of Mathematical Functions, 1046 pp., U.S. Dept. of Commerce, Washington, 1964.
- Alfvén, H., and C.-G. Fälthammar, Cosmical Electrodynamics, pp. 163-167, Clarendon Press, Oxford, 1963.
- Banks, P. M., C. R. Chappell, and A. F. Nagy, A new model for the interaction of auroral electrons with the atmosphere : spectral degradation, backscatter, optical emission, and ionization, J. Geophys. Res., 79, 1459, 1974.
- Banks, P. M., and T. E. Holzer, The polar wind, J. Geophys. Res., 73, 6846, 1968.
- Berko, F. W., and R. A. Hoffman, Dependence of field-aligned electron precipitation occurrence on season and altitude, J. Geophys. Res., 79, 3749, 1974.
- Block, L. P., Double layers, in Physics of the Hot Plasma in the Magnetosphere, pp.229-249, edited by B. Hultqvist and L. Stenflo, Plenum Press, N. Y., 1975.
- Chiu, Y. T., Self-consistent electrostatic field mapping in the high-latitude ionosphere, J. Geophys. Res., 79, 2790, 1974.
- CIRA, COSPAR International Reference Atmosphere, COSPAR Working Group 4, Akademie-Verlag, Berlin, 1972.
- Cornwall, J. M., Micropulsations and the outer radiation zone, J. Geophys. Res., 71, 2185, 1966.

PRECEDING PAGE BLANK-NOT FILMED

- Cornwall, J. M., F. V. Coroniti, and R. M. Thorne, Unified theory of SAR arc formation at the plasmapause, J. Geophys. Res., 76, 4428, 1971.
- DeForest, S. E., and C. E. McIlwain, Plasma clouds in the magnetosphere, J. Geophys. Res., 76, 3587, 1971.
- Evans, D. S., Precipitating electron fluxes formed by a magnetic field-aligned potential difference, J. Geophys. Res., 79, 2853, 1974.
- Evans, D. S., Evidence for the low altitude acceleration of auroral particles, in Physics of the Hot Plasma in the Magnetosphere, pp. 319-340, edited by B. Hultqvist and L. Stenflo, Plenum Press, N. Y., 1975.
- Evans, D. S., The acceleration of charged particles at low altitudes, in Physics of Solar Planetary Environments, pp. 730-739, edited by D. J. Williams, Am. Geophys. Union, Washington, 1976.
- Eviatar, A., A. M. Lenchek, and S. F. Singer, Distribution of density in an ion-exosphere of a non-rotating planet, Phys. Fluids, 7, 1775, 1964.
- Haerendel, G., E. Rieger, A. Valenzuela, H. Föppl, and H. Stenbaek-Nielsen, First observation of electrostatic acceleration of barium ions into the magnetosphere, preprint, Max Planck Institute for Physics and Astrophysics, Garching, 1976.
- Hoffman, J. H., W. H. Dodson, C. R. Lippincott, and H. D. Hammack, Initial ion composition results from the ISIS-2 satellite, J. Geophys. Res., 79, 4246, 1974.

- Hultqvist, B., H. Borg, W. Riedler, and P. Christopherson, Observation of a magnetic field-aligned anisotropy for 1 and 6 keV positive ions in the upper ionosphere, Planet. Space Sci., 19, 279, 1971.
- Kaufmann, R. L., D. N. Walker, and R. L. Arnoldy, Acceleration of auroral electrons in parallel electric fields, J. Geophys. Res., 81, 1673, 1976.
- Kennel, C. F., and H. E. Petschek, Limit on stably trapped particle fluxes, J. Geophys. Res., 71, 1, 1966.
- Kindel, J. M., and C. F. Kennel, Topside current instabilities, J. Geophys. Res., 76, 3055, 1971.
- Lemaire, J., and M. Scherer, Simple model for an ion-exosphere in an open magnetic field, Phys. Fluids, 14, 1683, 1971a.
- Lemaire, J., and M. Scherer, Kinetic models of the solar wind, J. Geophys. Res., 76, 7479, 1971b.
- Lemaire, J., and M. Scherer, Ionosphere-plasmasheet field-aligned currents and parallel electric fields, Planet. Space Sci., 22, 1485, 1974.
- Lemaire, J., and M. Scherer, Field-aligned distribution of plasma mantle and ionospheric plasmas, J. Atm. Terr. Phys., to be published, 1977.
- Lennartsson, W., On the magnetic mirroring as the basic cause of parallel electric fields, J. Geophys. Res., 81, 5583, 1976.
- Lennartsson, W., On high-latitude convection field inhomogeneities, parallel electric fields and inverted-V precipitation events, Planet. Space Sci., 25, 89, 1977.

- Mizera, P. F., D. R. Croley, Jr., and J. F. Fennell, Electron pitch-angle distributions in an inverted-'V' structure, Geophys. Res. Letters, 3, 149, 1976.
- Mozer, F. S., C. W. Carlson, M. K. Hudson, R. B. Torbert, B. Parady, J. Yatteau, and M. C. Kelley, Observation of paired electrostatic shocks in the polar magnetosphere, Phys. Rev. Letters, 38, 292, 1977.
- Papadopoulos, K., and T. Coffey, Nonthermal features of the auroral plasma due to precipitating electrons, J. Geophys. Res., 79, 674, 1974.
- Perkins, F. W., Plasma-wave instabilities in the ionosphere over the aurora, J. Geophys. Res., 73, 6631, 1968.
- Persson, H., Electric field along a magnetic line of force in a low-density plasma, Phys. Fluids, 6, 1756, 1963.
- Quon, B. H., and A. Y. Wong, Formation of potential double layers in plasmas, Phys. Rev. Letters, 37, 1393, 1976.
- Schulz, M., and H. C. Koons, Thermalization of colliding ion streams beyond the plasmopause, J. Geophys. Res., 77, 248, 1972.
- Shelley, E. G., R. D. Sharp, and R. G. Johnson, Satellite observation of an ionospheric acceleration mechanism, Geophys. Res. Letters, 3, 645, 1976.
- Swift, D. W., On the formation of auroral arcs and acceleration of auroral electrons, J. Geophys. Res., 80, 2096, 1975.

Winningham, J. D., T. W. Speiser, E. W. Hones, Jr., R. A. Jeffries,
W. H. Roach, D. S. Evans, and H. C. Stenbaek-Nielsen,
Rocket-borne measurements of the dayside cleft plasma:
The Tordo experiments, J. Geophys. Res., 82, in press, 1977.

Whipple, E. C., Jr., The signature of parallel electric fields in a collision-
less plasma. J. Geophys. Res., 82, 1525, 1977.

THE IVAN A. GETTING LABORATORIES

The Laboratory Operations of The Aerospace Corporation is conducting experimental and theoretical investigations necessary for the evaluation and application of scientific advances to new military concepts and systems. Versatility and flexibility have been developed to a high degree by the laboratory personnel in dealing with the many problems encountered in the nation's rapidly developing space and missile systems. Expertise in the latest scientific developments is vital to the accomplishment of tasks related to these problems. The laboratories that contribute to this research are:

Aerophysics Laboratory: Launch and reentry aerodynamics, heat transfer, reentry physics, chemical kinetics, structural mechanics, flight dynamics, atmospheric pollution, and high-power gas lasers.

Chemistry and Physics Laboratory: Atmospheric reactions and atmospheric optics, chemical reactions in polluted atmospheres, chemical reactions of excited species in rocket plumes, chemical thermodynamics, plasma and laser-induced reactions, laser chemistry, propulsion chemistry, space vacuum and radiation effects on materials, lubrication and surface phenomena, photo-sensitive materials and sensors, high precision laser ranging, and the application of physics and chemistry to problems of law enforcement and biomedicine.

Electronics Research Laboratory: Electromagnetic theory, devices, and propagation phenomena, including plasma electromagnetics; quantum electronics, lasers, and electro-optics; communication sciences, applied electronics, semiconducting, superconducting, and crystal device physics, optical and acoustical imaging; atmospheric pollution; millimeter wave and far-infrared technology.

Materials Sciences Laboratory: Development of new materials; metal matrix composites and new forms of carbon; test and evaluation of graphite and ceramics in reentry; spacecraft materials and electronic components in nuclear weapons environment; application of fracture mechanics to stress corrosion and fatigue-induced fractures in structural metals.

Space Sciences Laboratory: Atmospheric and ionospheric physics, radiation from the atmosphere, density and composition of the atmosphere, aurorae and airglow; magnetospheric physics, cosmic rays, generation and propagation of plasma waves in the magnetosphere; solar physics, studies of solar magnetic fields; space astronomy, x-ray astronomy; the effects of nuclear explosions, magnetic storms, and solar activity on the earth's atmosphere, ionosphere, and magnetosphere; the effects of optical, electromagnetic, and particulate radiations in space on space systems.

THE AEROSPACE CORPORATION
El Segundo, California
...

